User Manual for EPIPROD
Version 5.4, July 2005

James J. Kelly[1]

[1]*Department of Physics*
University of Maryland
College Park, MD 20742
jjkelly@physics.umd.edu

This manual describes the formalism and use of the program EPIPROD to compute observables and response functions for the electroproduction of pseudoscalar mesons upon nucleons. One can evaluate distributions with respect to various hadronic variables, expand response functions in Legendre series, or project multipole amplitudes using several reaction models. Calculations for pion production can be made using the unitary isobar model, the SAID partial-wave analysis, or by reading external files containing multipole amplitudes for the MAID2003, DMT, or SL models. Calculations for η production are presently limited to the isobar model. Response functions can be fit to data for the azimuthal and/or ϵ dependence of observables. Legendre coefficients can be fit to data for the angular dependence of response functions and/or observables. Alternatively, multipole amplitudes can be fit to data for many observables simultaneously. Many options are provided for representations of the response functions and conversion routines are provided for transformations between various representations of the reaction amplitudes. Subroutines are provided for using EPIPROD as an event generator for Monte Carlo simulation.

Contents

1. INTRODUCTION

The program EPIPROD calculates various quantities for the electroproduction of pseudoscalar mesons from nucleons in which the polarization of the recoil nucleon is detected. The original version of the program was written under my supervision by T.M. Payerle in 1992-1993 based, in part, upon an earlier program by R.W. Lourie [1, 2]. Since then the program has been extensively rewritten and extended by the present author and it continues to evolve in response to the needs of his experimental program. Among the features provided are:

- pion or eta electroproduction
- recoil or target polarization
- direct calculations using several models:
  - unitary isobar model
  - SAID [3]
  - MAID [4], DMT [5], SL [6], or other external model using interpolation within tabulated multipole amplitudes
- many conversion routines to transform between alternative representations of reaction amplitudes
- numerous options for definitions of response functions, polarization bases, and other conventions
- fitting experimental data using Legendre expansions of response functions
- fitting multipole amplitudes to experimental data for many quantities simultaneously
- fitting response functions to the azimuthal or ϵ dependencies of cross section and/or polarization data
- interface for use within the event generator for Monte Carlo simulations
- pseudodata testing

The organization of this manual is as follows. The kinematics of the meson electroproduction reactions are outlined in Sec. 2 and the observables and response functions are described in Sec. 3. Various representations of the reaction amplitudes are detailed in Sec. 4. Section 5 describes the available models. The program strategy and input conventions are described in Sec. 6. Sections 7 and 8 detail the input for direct calculations and for fitting procedures, respectively. These sections include sample input for most modes of operation. Section 9 details the input for various models. Section 10 describes the use of EPIPROD within a Monte Carlo event generator.

2. KINEMATICS

For clarity we underline four-vectors, use bold-face for three vectors, and ordinary typeface for scalars or for the magnitude of three vectors, such that $q = |\mathbf{q}|$. Unit vectors are denoted by carets, such that $\hat{\mathbf{q}}$ is a unit vector in the direction of $\mathbf{q}$.

In the one-photon exchange approximation, the kinematics of the electroproduction reaction are determined by the relationship

$$\underline{p}_i + \underline{q} = \underline{p}_f + \underline{p}_\pi$$

where $\underline{p}_i = (E_i, \mathbf{p}_i)$ and $\underline{p}_f = (E_f, \mathbf{p}_f)$ are the momenta of the target and recoil nucleons of mass m_i and m_f, $\underline{q} = (\omega, \mathbf{q}) = \underline{e}_i - \underline{e}_f$ is the momentum transfer brought by the virtual photon, and $\underline{p}_\pi = (E_\pi, \mathbf{p}_\pi)$ is the momentum of a meson of mass m_π, which can be a pion, eta, or other meson but denoted generally referred to as a *pion* hereafter. It is useful to define the Mandelstam invariants as

$$\begin{aligned} s &= (\underline{p}_i + \underline{q})^2 = (\underline{p}_f + \underline{p}_\pi)^2 && \text{(1a)} \\ t &= (\underline{p}_i - \underline{p}_f)^2 = (\underline{p}_\pi - \underline{q})^2 && \text{(1b)} \\ u &= (\underline{p}_i - \underline{p}_\pi)^2 = (\underline{p}_f - \underline{q})^2 && \text{(1c)} \end{aligned}$$

such that $s + t + u = m_i^2 + m_f^2 + m_\pi^2 - Q^2$ where $Q^2 = -q_\mu q^\mu$ is the spacelike virtuality of the photon. It is customary to express electroproduction amplitudes in the meson-nucleon center-of-mass frame, such that

$$\begin{aligned} s &= W^2 = (E_f + E_\pi)^2 && \text{(2a)} \\ t &= m_\pi^2 - Q^2 - 2E_\pi\omega + 2p_f q x && \text{(2b)} \\ u &= m_f^2 - Q^2 - 2E_f\omega - 2p_f q x && \text{(2c)} \end{aligned}$$

where W is the invariant mass, $x = \cos\theta_\pi$ is the cosine of the pion angle wrt $\mathbf{q}$, and $p_f = |\mathbf{p}_f| = |\mathbf{p}_\pi|$ is the recoil momentum in the center-of-mass.

It will be useful to define

$$q_0 = \frac{W^2 - m_i^2}{2W} \tag{3}$$

as the momentum needed by a real photon to excite a state with invariant mass W and

$$\begin{aligned} q_{0R} &= \frac{W_R^2 - m_i^2}{2W_R} && \text{(4a)} \\ k_R &= \frac{1}{2W_R}\left[(W_R^2 - m_f^2 - m_\pi^2)^2 - (2m_f m_\pi)^2\right]^{1/2} && \text{(4b)} \end{aligned}$$

as pion and real-photon momenta for a resonance at $W = W_R$.

3. OBSERVABLES

3.1. Cross section

The differential cross section for recoil polarization in the pion electroproduction reaction $p(\vec{e}, e'\vec{N})\pi$ can be expressed in the form

$$\frac{d^5\sigma}{dk_f d\Omega_e d\Omega^*} = \Gamma_\gamma \bar{\sigma}\left[1 + hA + \mathbf{\Pi}\cdot\boldsymbol{S}\right] \tag{5}$$

where $\bar{\sigma}$ is the unpolarized cross section, h is the electron helicity, $\boldsymbol{S}$ is the spin direction for the recoil nucleon, A is the beam analyzing power, $\mathbf{\Pi}$ is the recoil polarization coefficient,

$$\Gamma_\gamma = \frac{\alpha}{2\pi^2}\frac{k_f}{k_i}\frac{k_\gamma}{Q^2}\frac{1}{1-\epsilon} \tag{6}$$

is the virtual photon flux for initial (final) electron momenta k_i (k_f), $\epsilon = \left(1 + 2\frac{\mathbf{q}^2}{Q^2}\tan^2\frac{\theta_e}{2}\right)^{-1}$ is the transverse polarization of the virtual photon, θ_e is the electron scattering angle, and $k_\gamma = (W^2 - m_p^2)/2m_p$ is the laboratory energy a real photon would need to excite the same transition. Note that electron kinematics and solid angle $d\Omega_e$ are normally expressed in the lab frame while hadron kinematics and nucleon solid angle $d\Omega^*$ are expressed in the πN cm frame.

A similar expression applies when the target is polarized and the recoil polarization is unobserved, except that $\boldsymbol{S}$ then represents the target direction and $\mathbf{\Pi}$ is interpreted as the target polarization coefficient. Simultaneous target and recoil polarization has not been implemented.

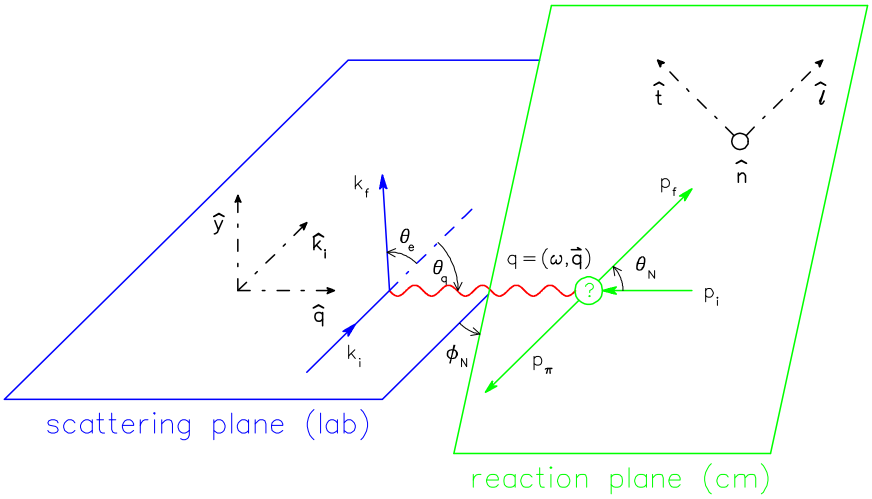

FIG. 1: Kinematics of the $p(\vec{e}, e'\vec{N})\pi$ reaction and the polarization basis vectors for the cm reaction basis.

3.2. Recoil polarization

Polarization observables $\boldsymbol{\Pi} = \boldsymbol{P} + h\boldsymbol{P}'$ can be separated into helicity-independent and helicity-dependent contributions denoted $\boldsymbol{P}$ and $\boldsymbol{P}'$, respectively. The components of these vectors can be expressed in several alternative bases either in the cm or lab frames. The calculation of recoil polarization observables always starts with the cm reaction basis, $(\hat{t}, \hat{n}, \hat{\ell})$, and then matrices listed in Appendix B are used to transform those observables to the basis requested by the user. The kinematics of the $p(\vec{e}, e'\vec{p})\pi^0$ reaction and the orientation of the basis vectors for the cm reaction basis are illustrated in Fig. 1, with electron scattering shown in the lab frame and the πN final state in the cm frame.

3.2.1. Polarization bases for cm frame

Recoil polarization is usually calculated with respect to a *cm reaction basis* defined by

$$\hat{\ell} = \hat{p}_N \tag{7a}$$
$$\hat{n} \propto \hat{q} \wedge \hat{\ell} \tag{7b}$$
$$\hat{t} = \hat{n} \wedge \hat{\ell} \tag{7c}$$

where $\hat{p}_N$ is the recoil nucleon direction in the cm frame. This basis is well defined when θ_N is not equal to $0°$ or $180°$, but difficulties arise when $\hat{q}$ and $\hat{p}_N$ are either parallel or antiparallel and ϕ_N loses physical meaning. These cases are conventionally handled by first rotating the reaction plane to ϕ_N as it would be in non-parallel kinematics, and then taking the limit $\theta \to 0°$ or $\theta \to 180°$ as required. Note that since the basis vectors $\hat{t}$ and $\hat{n}$ reverse directions when $\phi \longrightarrow \phi + \pi$, the corresponding components of the recoil polarizations also tend to reverse sign even when there is no physical asymmetry with respect to ϕ; this behavior is simply an artifact of the basis.

An option is provided to replace $\hat{p}_N$ by $\hat{p}_\pi$ in Eq. (7), thereby reversing the directions of $\hat{\ell}$ and $\hat{n}$ while leaving $\hat{t}$ unchanged. This option was intended to provide compatibility with some other authors, such as Ref. [4], that base most variables upon pion coordinates. However, MAID does not reverse $\hat{n}$ when taking $\hat{\ell}$ along $\hat{p}_N$; consequently, these codes still have opposite signs for $\hat{n}$ and $\hat{t}$ with this option.

It is also useful to define a *photon basis*

$$\hat{z} = \hat{q} \tag{8a}$$
$$\hat{y} \propto \hat{k}_i \wedge \hat{k}_f \tag{8b}$$
$$\hat{x} = \hat{y} \wedge \hat{z} \tag{8c}$$

in which $\hat{z}$ is along the virtual photon and $\hat{y}$ is normal to the electron scattering frame. This basis is particularly useful for small scattering angles approaching the limit of parallel kinematics where it is difficult to determine the orientation of the reaction plane accurately.

3.2.2. Polarization bases for lab frame

The transformation of polarization from the cm to the lab frame requires a Wigner rotation [7, 8] that is discussed in Appendix A. One can then express the polarization is several bases. For the *lab reaction* basis we define

$$\hat{L} = \hat{p}_N \tag{9a}$$
$$\hat{N} \propto \hat{q} \wedge \hat{L} \tag{9b}$$
$$\hat{S} = \hat{N} \wedge \hat{L} \tag{9c}$$

where $\hat{p}_N$ is now the nucleon momentum direction in the lab frame.

We also provide a *polarimeter basis* defined by

$$\hat{f} = \hat{p}_N \tag{10a}$$
$$\hat{d} \propto \hat{y} \wedge \hat{f} \tag{10b}$$
$$\hat{e} = \hat{f} \wedge \hat{d} \tag{10c}$$

where here $\hat{p}_N$ is expressed in the laboratory frame. This basis offers the advantage that neither $\hat{d}$ nor $\hat{e}$ changes sign abruptly as $\hat{\ell}$ passes through $\hat{q}$, so that polarization components display a smoother angular dependence than in the reaction basis. On the other hand, the response functions do not separate as cleanly.

Finally, we define a *lab basis*

$$\hat{c} = \hat{k}_i \tag{11a}$$
$$\hat{b} \propto \hat{k}_i \wedge \hat{k}_f \tag{11b}$$
$$\hat{a} = \hat{b} \wedge \hat{c} \tag{11c}$$

that has $\hat{c}$ along the electron beam direction, $\hat{b}$ normal to the electron scattering plane, and $\hat{a}$ transverse to the beam in the scattering plane.

3.2.3. Reaction basis

It is also useful to define a *reaction basis*

$$\hat{z} = \hat{q} \tag{12a}$$
$$\hat{n} \propto \hat{q} \wedge \hat{p}_N \tag{12b}$$
$$\hat{m} = \hat{n} \wedge \hat{z} \tag{12c}$$

that is the same for both cm and lab frames and has $\hat{n}$ normal to the reaction plane. This basis is most useful for target polarization but is also available for recoil polarization. Note that the reaction and photon bases coincide for $\phi_N = 0$, but $\hat{n} = -\hat{y}$, $\hat{m} = -\hat{t}$ for $\phi_N = \pi$. An option is provided here also to replace $\hat{p}_N$ by $\hat{p}_\pi$ in Eq. (12). The effect is to reverse $\hat{m}$ and $\hat{n}$ and provides the basis labelled (Px,Py,Pz) by MAID [4].

3.3. Target polarization

The options for target polarization are more limited because the recoil momentum is less relevant. Therefore, we consider only the reaction, photon, or lab bases given by Eqs. (12,8,11) respectively. The default is Eq. (12), which is used for internal calculations. Tranformations from the reaction basis to the desired output basis are also listed in Appendix B.

3.4. Response functions

It is well-known that if the polarization vectors are expressed relative to a basis with $\hat{n}$ normal to the reaction plane, the azimuthal dependence can be extracted and the observables can be decomposed into kinematical factors, ν_α, which depend only upon electron kinematics and response functions, $\mathcal{W}_\alpha(x, W, Q^2)$ which carry the hadronic information. For kinematic factors α identifies the appropriate element of the density matrix for the polarization of the virtual photon, while for response functions it also identifies the target or recoil polarization component. This decomposition

$$
\begin{aligned}
\bar{\sigma} &= \nu_0 \left[\nu_L \mathcal{W}_L + \nu_T \mathcal{W}_T + \nu_{LT} \mathcal{W}_{LT} \cos\phi + \nu_{TT} \mathcal{W}_{TT} \cos 2\phi\right] && \text{(13a)}\\
A\bar{\sigma} &= \nu_0 \left[\nu'_{LT} \mathcal{W}'_{LT} \sin\phi\right] && \text{(13b)}\\
P_t\bar{\sigma} &= \nu_0 \left[\nu_{LT} \mathcal{W}^t_{LT} \sin\phi + \nu_{TT} \mathcal{W}^t_{TT} \sin 2\phi\right] && \text{(13c)}\\
P_n\bar{\sigma} &= \nu_0 \left[\nu_L \mathcal{W}^n_L + \nu_T \mathcal{W}^n_T + \nu_{LT} \mathcal{W}^n_{LT} \cos\phi + \nu_{TT} \mathcal{W}^n_{TT} \cos 2\phi\right] && \text{(13d)}\\
P_\ell\bar{\sigma} &= \nu_0 \left[\nu_{LT} \mathcal{W}^\ell_{LT} \sin\phi + \nu_{TT} \mathcal{W}^\ell_{TT} \sin 2\phi\right] && \text{(13e)}\\
P'_t\bar{\sigma} &= \nu_0 \left[\nu'_{LT} \mathcal{W}'^t_{LT} \cos\phi + \nu'_{TT} \mathcal{W}'^t_{TT}\right] && \text{(13f)}\\
P'_n\bar{\sigma} &= \nu_0 \left[\nu'_{LT} \mathcal{W}'^n_{LT} \sin\phi\right] && \text{(13g)}\\
P'_\ell\bar{\sigma} &= \nu_0 \left[\nu'_{LT} \mathcal{W}'^\ell_{LT} \cos\phi + \nu'_{TT} \mathcal{W}'^\ell_{TT}\right] && \text{(13h)}
\end{aligned}
$$

can be obtained using the reaction basis or any other obtained by rotation about $\hat{n}$, in which case the $\hat{\ell}$ and $\hat{t}$ components become mixed accordingly.

For many purposes, it is useful to extract factors of $\sin\theta$ from the response functions, such that

$$
\begin{aligned}
\bar{\sigma} &= \nu_0 \left[\nu_L R_L + \nu_T R_T + \nu_{LT} R_{LT} \sin\theta\cos\phi + \nu_{TT} R_{TT} \sin^2\theta \cos 2\phi\right] && \text{(14a)}\\
A\bar{\sigma} &= \nu_0 \left[\nu'_{LT} R'_{LT} \sin\theta \sin\phi\right] && \text{(14b)}\\
P_t\bar{\sigma} &= \nu_0 \left[\nu_{LT} R^t_{LT} \sin\phi + \nu_{TT} R^t_{TT} \sin\theta \sin 2\phi\right] && \text{(14c)}\\
P_n\bar{\sigma} &= \nu_0 \left[(\nu_L R^n_L + \nu_T R^n_T)\sin\theta + \nu_{LT} R^n_{LT} \cos\phi + \nu_{TT} R^n_{TT} \sin\theta \cos 2\phi\right] && \text{(14d)}\\
P_\ell\bar{\sigma} &= \nu_0 \left[\nu_{LT} R^\ell_{LT} \sin\theta \sin\phi + \nu_{TT} R^\ell_{TT} \sin^2\theta \sin 2\phi\right] && \text{(14e)}\\
P'_t\bar{\sigma} &= \nu_0 \left[\nu'_{LT} R'^t_{LT} \cos\phi + \nu'_{TT} R'^t_{TT} \sin\theta\right] && \text{(14f)}\\
P'_n\bar{\sigma} &= \nu_0 \left[\nu'_{LT} R'^n_{LT} \sin\phi\right] && \text{(14g)}\\
P'_\ell\bar{\sigma} &= \nu_0 \left[\nu'_{LT} R'^\ell_{LT} \sin\theta\cos\phi + \nu'_{TT} R'^\ell_{TT}\right] && \text{(14h)}
\end{aligned}
$$

are expressed in terms of *reduced* response functions, R_α. The reduced response functions can then be expressed as polynomials in x or as Legendre expansions

$$R_\alpha(x, W, Q^2) = \sum_{n=0}^{\infty} A^\alpha_n(W, Q^2) P_n(x) = \sum_{n=0}^{\infty} B^\alpha_n(W, Q^2) x^n \tag{15}$$

that should should converge quickly for modest (W, Q^2). These expansions are closely related to those used to report experimental data, *e.g.* Ref. [9, 10]. Another advantage of this representation is that the accuracy of acceptance averaging in data analysis should be improved by including explicitly all angular dependencies that are independent of the reaction dynamics.

It is also useful to define inclusive cross sections

$$\sigma_\alpha = \int d\Omega\, R_\alpha = 4\pi A^\alpha_0 \tag{16}$$

based upon each of the response functions.

Regrettably, no single convention for the signs and normalizations of the response functions has gained wide acceptance. Therefore, `EPIPROD` provides several choices listed in Table I. Most of the code is based upon the internal representation. The standard or default representation provides the simplest multiple expansions. Other representations are identified by the author that uses it and typical references; however,

TABLE I: Kinematic factors for several conventional definitions of the response functions.

`rsfns_type`	Ref.	ϕ	ν_0	ν_L	ν_T	ν_{LT}	ν_{TT}	ν'_{LT}	ν'_{TT}
`'internal'`		ϕ_π	$\frac{k}{q_0}$	ϵ	1	$\sqrt{\epsilon(1+\epsilon)}$	ϵ	$\sqrt{\epsilon(1-\epsilon)}$	$\sqrt{1-\epsilon^2}$
`'standard'`		ϕ_π	$\frac{k}{q_0}$	ϵ_S	1	$\sqrt{2\epsilon_S(1+\epsilon)}$	ϵ	$\sqrt{2\epsilon_S(1-\epsilon)}$	$\sqrt{1-\epsilon^2}$
`'DT'`	[11]	ϕ_π	$\frac{k}{q_0}$	ϵ_L	1	$\sqrt{2\epsilon_L(1+\epsilon)}$	ϵ	$\sqrt{2\epsilon_L(1-\epsilon)}$	$\sqrt{1-\epsilon^2}$
`'Lourie'`	[1, 2]	ϕ_N	$\frac{k}{q_0}$	ϵ_S	1	$\sqrt{2\epsilon_S(1+\epsilon)}$	ϵ	$\sqrt{2\epsilon_S(1-\epsilon)}$	$\sqrt{1-\epsilon^2}$
`'NL'`	[12]	ϕ_π	1	ϵ	1	$\sqrt{2\epsilon(1+\epsilon)}$	ϵ	$\sqrt{2\epsilon(1-\epsilon)}$	$\sqrt{1-\epsilon^2}$

some authors (including this one) have used several variations even within their own work. Other options can be added to the subroutine `vfactors` if needed. Some options employ longitudinal or scalar polarization parameters related to ϵ by

$$\epsilon_S = \frac{Q^2}{q^2}\epsilon \qquad \epsilon_L = \frac{Q^2}{\omega^2}\epsilon \; . \tag{17}$$

where (ω, q) are evaluated in the cm frame. We do not recommend using ϵ_L because ω crosses zero as Q^2 increases. The overall factor ν_0 permits phase-space factors to be extracted from the response functions, thereby simplifying multipole expansions. This factor is usually taken as the ratio between the cm momentum in the final state and the cm momentum a real photon needs for the same transition, such that $\nu_0 = k/q_0$ where

$$k^2 = \frac{(W^2 + m_\pi^2 - m_p^2)^2}{4W^2} - m_\pi^2 \tag{18a}$$

$$q_0 = \frac{W^2 - m_p^2}{2W} \tag{18b}$$

3.5. Asymmetries

Upon request, EPIPROD will also print a set of azimuthal asymmetries defined as ratios between the linear combinations of partial cross sections for several values of ϕ and a similar combinations of unpolarized cross sections for the same values of ϕ. These asymmetries are designed to isolate one response function in the numerator, relative to a suitable cross section in the denominator. Measurements of this type have the advantage of reduced dependencies upon uncertainties in luminosity, deadtimes, efficiencies, and other normalization uncertainties, especially if the measurements for various ϕ values are simultaneously, but still depend upon acceptance models. This method has been used for the left-right cross section asymmetry, which is related to $\mathcal{W}_{LT}$, *e.g.* Refs. [13, 14], but has not been exploited for the other quantities listed below.

Values of ϕ_π are given as subscripts in the following definitions.

$$\alpha_{LT} = \frac{\bar\sigma_\pi - \bar\sigma_0}{\bar\sigma_\pi + \bar\sigma_0} = -\frac{\nu_{LT}\mathcal{W}_{LT}}{\nu_L\mathcal{W}_L + \nu_T\mathcal{W}_T + \nu_{TT}\mathcal{W}_{TT}} \tag{19a}$$

$$\alpha^n_{LT} = \frac{(P_n\bar\sigma)_\pi - (P_n\bar\sigma)_0}{\bar\sigma_\pi + \bar\sigma_0} = -\frac{\nu_{LT}\mathcal{W}^n_{LT}}{\nu_L\mathcal{W}_L + \nu_T\mathcal{W}_T + \nu_{TT}\mathcal{W}_{TT}} \tag{19b}$$

$$\alpha^\ell_{LT} = \frac{(P_\ell\bar\sigma)_{\pi/2} - (P_\ell\bar\sigma)_{-\pi/2}}{\bar\sigma_{\pi/2} + \bar\sigma_{-\pi/2}} = \frac{\nu_{LT}\mathcal{W}^\ell_{LT}}{\nu_L\mathcal{W}_L + \nu_T\mathcal{W}_T - \nu_{TT}\mathcal{W}_{TT}} \tag{19c}$$

$$\alpha^t_{LT} = \frac{(P_t\bar\sigma)_{\pi/2} - (P_t\bar\sigma)_{-\pi/2}}{\bar\sigma_{\pi/2} + \bar\sigma_{-\pi/2}} = \frac{\nu_{LT}\mathcal{W}^t_{LT}}{\nu_L\mathcal{W}_L + \nu_T\mathcal{W}_T - \nu_{TT}\mathcal{W}_{TT}} \tag{19d}$$

$$\alpha'_{LT} = \frac{\bar\sigma_{3\pi/2} - \bar\sigma_{\pi/2}}{\bar\sigma_{3\pi/2} + \bar\sigma_{\pi/2}} = -\frac{\nu'_{LT}\mathcal{W}'_{LT}}{\nu_L\mathcal{W}_L + \nu_T\mathcal{W}_T - \nu_{TT}\mathcal{W}_{TT}} \tag{19e}$$

$$\alpha'^n_{LT} = \frac{(P'_n\bar\sigma)_{3\pi/2} - (P'_n\bar\sigma)_{\pi/2}}{\bar\sigma_{3\pi/2} + \bar\sigma_{\pi/2}} = -\frac{\nu'_{LT}\mathcal{W}'^n_{LT}}{\nu_L\mathcal{W}_L + \nu_T\mathcal{W}_T - \nu_{TT}\mathcal{W}_{TT}} \tag{19f}$$

$$\alpha'^\ell_{LT} = \frac{(P'_\ell\bar\sigma)_\pi - (P'_\ell\bar\sigma)_0}{\bar\sigma_\pi + \bar\sigma_0} = -\frac{\nu_{LT}\mathcal{W}'^\ell_{LT}}{\nu_L\mathcal{W}_L + \nu_T\mathcal{W}_T + \nu_{TT}\mathcal{W}_{TT}} \tag{19g}$$

$$\alpha'^t_{LT} = \frac{(P'_t\bar\sigma)_\pi - (P'_t\bar\sigma)_0}{\bar\sigma_\pi + \bar\sigma_0} = -\frac{\nu_{LT}\mathcal{W}'^t_{LT}}{\nu_L\mathcal{W}_L + \nu_T\mathcal{W}_T + \nu_{TT}\mathcal{W}_{TT}} \tag{19h}$$

$$\alpha_{TT} = \frac{\bar\sigma_0 - \bar\sigma_{\pi/2} + \bar\sigma_\pi - \bar\sigma_{3\pi/2}}{\bar\sigma_0 + \bar\sigma_{\pi/2} + \bar\sigma_\pi + \bar\sigma_{3\pi/2}} = \frac{\nu_{TT}\mathcal{W}_{TT}}{\nu_L\mathcal{W}_L + \nu_T\mathcal{W}_T} \tag{19i}$$

$$\alpha^n_{TT} = \frac{(P_n\bar\sigma)_0 - (P_n\bar\sigma)_{\pi/2} + (P_n\bar\sigma)_\pi - (P_n\bar\sigma)_{3\pi/2}}{\bar\sigma_0 + \bar\sigma_{\pi/2} + \bar\sigma_\pi + \bar\sigma_{3\pi/2}} = \frac{\nu_{TT}\mathcal{W}^n_{TT}}{\nu_L\mathcal{W}_L + \nu_T\mathcal{W}_T} \tag{19j}$$

$$\alpha^\ell_{TT} = \frac{(P_\ell\bar\sigma)_{\pi/4} - (P_\ell\bar\sigma)_{3\pi/4} + (P_\ell\bar\sigma)_{5\pi/4} - (P_\ell\bar\sigma)_{7\pi/4}}{\bar\sigma_{\pi/4} + \bar\sigma_{3\pi/4} + \bar\sigma_{5\pi/4} + \bar\sigma_{7\pi/4}} = \frac{\nu_{TT}\mathcal{W}^\ell_{TT}}{\nu_L\mathcal{W}_L + \nu_T\mathcal{W}_T} \tag{19k}$$

$$\alpha^t_{TT} = \frac{(P_t\bar\sigma)_{\pi/4} - (P_t\bar\sigma)_{3\pi/4} + (P_t\bar\sigma)_{5\pi/4} - (P_t\bar\sigma)_{7\pi/4}}{\bar\sigma_{\pi/4} + \bar\sigma_{3\pi/4} + \bar\sigma_{5\pi/4} + \bar\sigma_{7\pi/4}} = \frac{\nu_{TT}\mathcal{W}^t_{TT}}{\nu_L\mathcal{W}_L + \nu_T\mathcal{W}_T} \tag{19l}$$

$$\alpha'^\ell_{TT} = \frac{(P'_\ell\bar\sigma)_\pi + (P'_\ell\bar\sigma)_0}{\bar\sigma_\pi + \bar\sigma_0} = \frac{\nu_{TT}\mathcal{W}'^\ell_{TT}}{\nu_L\mathcal{W}_L + \nu_T\mathcal{W}_T + \nu_{TT}\mathcal{W}_{TT}} \tag{19m}$$

$$\alpha'^t_{TT} = \frac{(P'_t\bar\sigma)_\pi + (P'_t\bar\sigma)_0}{\bar\sigma_\pi + \bar\sigma_0} = \frac{\nu_{TT}\mathcal{W}'^t_{TT}}{\nu_L\mathcal{W}_L + \nu_T\mathcal{W}_T + \nu_{TT}\mathcal{W}_{TT}} \tag{19n}$$

Although it is possible to eliminate $\mathcal{W}_{TT}$ from all of the denominators using slightly more elaborate linear combinations, we decided to employ the simplest combinations that provide the desired numerators even if some of the denominators are more complicated assuming that if any asymmetries beyond α_{LT} are measured in the future the minimum number of measurements would be employed. Most users will probably want to suppress the output of asymmetries, but these quantities have been retained in the code for academic reasons.

3.6. Quadrupole ratios

Some modes also output the quadrupole ratios

$$R_{EM} = \mathrm{Re}(E_{1+}/M_{1+}) \tag{20a}$$

$$R_{SM} = \mathrm{Re}(S_{1+}/M_{1+}) \tag{20b}$$

labeled EMR and SMR, respectively. These are most interesting in the immediate vicinity of the $P_{33}(1232)$ resonance, but are evaluated for any W. These quantities are evaluated for a particular channel without projection with respect to isospin.

An option is provided to evaluate this quantity phenomenologically also. For Legendre fits to the differential equation, we apply the traditional estimators

$$\tilde{R}_{EM} \approx \frac{3A_2^{L+T} - 2A_0^{TT}}{12A_0^{L+T}} \tag{21a}$$

$$\tilde{R}_{SM} \approx \frac{A_1^{LT}}{3A_0^{L+T}} \tag{21b}$$

obtained under the assumptions of *sp* truncation and M_{1+} dominance. The values at $W = M_\Delta$ approximate the $N \to \Delta(1232)$ quadrupole ratios for a specific reaction channel. Isolating the pure isospin-(3/2) contributions requires data for several reactions. Alternatively, `EPIPROD` multipole analyses report

$$R_{EM} = \frac{\mathrm{Re}E_{1+}^* M_{1+}}{|M_{1+}|^2} = \frac{\mathrm{Re}E_{1+}\mathrm{Re}M_{1+} + \mathrm{Im}E_{1+}\mathrm{Im}M_{1+}}{\mathrm{Re}M_{1+}\mathrm{Re}M_{1+} + \mathrm{Im}M_{1+}\mathrm{Im}M_{1+}} \tag{22a}$$

$$R_{SM} = \frac{\mathrm{Re}S_{1+}^* M_{1+}}{|M_{1+}|^2} = \frac{\mathrm{Re}S_{1+}\mathrm{Re}M_{1+} + \mathrm{Im}S_{1+}\mathrm{Im}M_{1+}}{\mathrm{Re}M_{1+}\mathrm{Re}M_{1+} + \mathrm{Im}M_{1+}\mathrm{Im}M_{1+}} \tag{22b}$$

directly. Note that M_Δ is sometimes defined by the condition

$$W \to M_\Delta \Longrightarrow \mathrm{Re}M_{1+}^{(3/2)} \to 0 \tag{23}$$

such that

$$R_{EM}^{(3/2)} = \left(\frac{\mathrm{Im}E_{1+}^{(3/2)}}{\mathrm{Im}M_{1+}^{(3/2)}} \right)_{W=M_\Delta} \tag{24a}$$

$$R_{SM}^{(3/2)} = \left(\frac{\mathrm{Im}S_{1+}^{(3/2)}}{\mathrm{Im}M_{1+}^{(3/2)}} \right)_{W=M_\Delta} \tag{24b}$$

but we prefer to retain the W dependencies in Eq. (22) because the sign change in a specific isospin channel is difficult to identify experimentally.

Note that the subroutines for both Legendre and multipole analysis of quadrupole ratios perform error propagation using the covariance matrix. However, no provision is available yet for analyzing the W dependence of these ratio or performing isospin decomposition.

3.7. Special quantities for parallel kinematics

The azimuthal symmetry of parallel kinematics requires the response functions for transverse components of recoil polarization to satisfy

$$R_{LT}^t = \mp R_{LT}^n \ , \ R_{LT}'^t = \pm R_{LT}'^n \tag{25}$$

where the signs are correlated with $x = \pm 1$ throughout this section. Furthermore, there are only four independent response functions because only two helicity amplitudes survive in parallel kinematics. Thus, the observables can be represented in the photon basis defined in Eq. (8) as

$$\bar{\sigma} = \nu_0 R_{L+T} = \nu_0(1 + \nu_L r^2) R_T \tag{26a}$$

$$P_x' \bar{\sigma} = \pm \nu_0 \nu_{LT}' R_{LT}'^t = \mp \nu_0 \nu_{LT}' r R_T \cos\delta \tag{26b}$$

$$P_y \bar{\sigma} = -\nu_0 \nu_{LT} R_{LT}^n = \mp \nu_0 \nu_{LT} r R_T \sin\delta \tag{26c}$$

$$P_z' \bar{\sigma} = \mp \nu_0 \nu_{TT}' R_{TT}'^\ell = \nu_0 \nu_{TT}' R_T \tag{26d}$$

Similarly, the response functions with standard `EPIPROD` conventions

$$R_L = |L|^2 \tag{27a}$$

$$R_T = |T|^2 \tag{27b}$$

$$R_{LT}'^t = -r R_T \cos\delta \tag{27c}$$

$$R_{LT}^n = \pm r R_T \sin\delta \tag{27d}$$

$$R_{TT}'^\ell = \mp R_T \tag{27e}$$

can be represented in terms of the transverse and longitudinal amplitudes for parallel kinematics

$$T_\pm = \mathcal{F}_2 \mp \mathcal{F}_1 \tag{28a}$$
$$L_\pm = \frac{q}{\omega}(\mathcal{F}'_5 \pm \mathcal{F}'_6) \tag{28b}$$

and where the $\mathcal{F}_i$ represent CGLN amplitudes.

Finally, it is useful to describe the ratio between longitudinal and transverse amplitudes as

$$\frac{L}{T} = re^{i\delta} = \frac{\pm R'^{t}_{LT} - iR^{n}_{LT}}{R'^{\ell}_{TT}} \tag{29}$$

where the subscripts $\pm$ remain implicit. The relationship between R'^{ℓ}_{TT} and R_T in parallel kinematics is a special property of $(\vec{e}, e'\vec{N})$ reactions between spin one-half states, such as pion electroproduction on the nucleon, that depends only upon parity conservation and the dominance of one-photon exchange. An important advantage of polarization measurements over Rosenbluth separation is that one obtains the relative phase in addition to the relative magnitude of the longitudinal and transverse amplitudes.

The transverse and longitudinal amplitudes for parallel kinematics can be expanded in multipoles according to

$$T_+ = -\frac{1}{2}\sum_\ell \left(\ell(\ell+1)(M_{\ell+} - M_{\ell-}) + (\ell+1)(\ell+2)E_{\ell+} + \ell(\ell-1)E_{\ell-}\right) \tag{30a}$$
$$T_- = \frac{1}{2}\sum_\ell (-)^\ell \left(\ell(\ell+1)(M_{\ell+} - M_{\ell-}) + (\ell+1)(\ell+2)E_{\ell+} + \ell(\ell-1)E_{\ell-}\right) \tag{30b}$$
$$L_+ = \frac{q}{Q}\sum_\ell \left((\ell+1)^2 S_{\ell+} + \ell^2 S_{\ell-}\right) \tag{30c}$$
$$L_- = \frac{q}{Q}\sum_\ell (-)^\ell \left((\ell+1)^2 S_{\ell+} + \ell^2 S_{\ell-}\right) \tag{30d}$$

Thus, if one limits the expansions to s- and p-waves one finds

$$T_\pm \approx \mp E_{0+} - M_{1+} + M_{1-} - 3E_{1+} + \ldots \tag{31a}$$
$$\frac{Q}{q}L_\pm \approx S_{0+} \pm 4S_{1+} \pm S_{1-} + \ldots \tag{31b}$$

Although one cannot rigorously separate the multipole contributions to the longitudinal and transverse amplitudes using only polarization measurements for parallel and/or antiparallel kinematics, useful estimates can be obtained under some circumstances. Two examples are discussed in Secs. 3.7.2 and 3.7.3.

3.7.1. Estimators for R_L/R_T

Kelly [15] proposed a method for measurement of r and δ based upon P'_z for parallel kinematics that provides the ratio

$$\mathcal{R} = \frac{R_L}{R_T} = \left|\frac{L}{T}\right|^2 = r^2 \tag{32}$$

between longitudinal and transverse response functions without Rosenbluth separation. An advantage of this method is that it does not require the helicity-independent normal polarization, P_y, which may be vulnerable to false asymmetries in the polarimeter. Schmieden and Tiator [16] then proposed two alternative methods, one based upon P'_x and P_y and another using all three components, and stated explicitly the model-independent consistency relation

$$|R'^{t}_{LT}|^2 + |R^{n}_{LT}|^2 = R_L R_T \tag{33}$$

implicit in Eq. (26). Their methods offered better error propagation for the kinematics of Ref. [17]. However, neither of these proposals considered the effects of acceptance averaging or nonuniformities in the ϕ acceptance. These issues are important because it is impossible to achieve strictly parallel kinematics.

A more practical method uses the Legendre fit to response functions to project those quantities to $x = \pm 1$, thereby minimizing the effects of acceptance averaging and circumventing the requirement of uniform ϕ acceptance for direct measurement of polarization components. Thus, we obtain three estimators

$$\mathcal{R}_\ell = -(1 \pm \frac{R_{L+T}}{R'^{\ell}_{TT}})/\nu_L \tag{34a}$$

$$\mathcal{R}_{tn\ell} = \frac{|R'^{t}_{LT}|^2 + |R'^{n}_{LT}|^2 + |R^{t}_{LT}|^2 + |R^{n}_{LT}|^2}{2|R'^{\ell}_{TT}|^2} \tag{34b}$$

$$\mathcal{R}_{tn} = \frac{1 - 2\nu_L\chi^2_\perp - \sqrt{1 - 4\nu_L\chi^2_\perp}}{2\nu_L^2\chi^2_\perp} \tag{34c}$$

where

$$\chi^2_\perp = \frac{|R'^{t}_{LT}|^2 + |R'^{n}_{LT}|^2 + |R^{t}_{LT}|^2 + |R^{n}_{LT}|^2}{2|R_{L+T}|^2} \tag{35}$$

should satisfy the inequality

$$\chi^2_\perp \leq (4\nu_L)^{-1} \tag{36}$$

Note that we have used the rotational invariance represented by Eq. (25) to symmetrize the numerators of $\mathcal{R}_{tn\ell}$ and $\chi^2_\perp$. An advantage of $\mathcal{R}_{tn\ell}$ is that it is insensitive to the analyzing power of the polarimeter.

These estimators are analogous to those proposed by Refs. [15, 16] in terms of polarization measurements and should all be equivalent to $\mathcal{R}$ if the data for response functions are consistent with the azimuthal and dynamical symmetries for parallel kinematics. Thus, it is also useful to define the quantities

$$\alpha = \mp\frac{R^{t}_{LT}}{R^{n}_{LT}} \tag{37a}$$

$$\alpha' = \mp\frac{R'^{t}_{LT}}{R'^{n}_{LT}} \tag{37b}$$

$$\beta = \mp\frac{2R'^{\ell}_{TT}}{\nu_L}\frac{R_{L+T} \mp R'^{\ell}_{TT}}{|R'^{t}_{LT}|^2 + |R'^{n}_{LT}|^2 + |R^{t}_{LT}|^2 + |R^{n}_{LT}|^2} \tag{37c}$$

to test those symmetries; all should have unit value if the symmetry relations are satisfied. The quantities α and α' measure the geometrical consistency of the separation of response functions using the azimuthal dependence of polarization measurements while β is a dynamical symmetry that tests the dominance of one-photon exchange and the limitation of the reaction to two helicity amplitudes. Thus, the output for α, α', and β provided for Legendre fits to data for response functions provides useful tests of the internal consistency of the data or, possibly, the reliability of one photon exchange for this reaction. Multipole fits satisfy these consistency tests automatically, but comparsion of the estimated uncertainties with those for Legendre fits can be enlightening.

Finally, the relative phase between longitudinal and transverse amplitudes is given by quadrant-sensitive arctangent function

$$\delta_\pm = \arctan\left(-R'^{t}_{LT}, \pm R^{n}_{LT}\right) \tag{38}$$

where the argument order is (horizontal,vertical). The same definitions are used for both Legendre and multipole fits.

3.7.2. Estimators for S_{0+}/E_{0+}

Sufficiently near threshold we may be able to neglect p waves such that

$$W \gtrsim m_N + m_\pi \Longrightarrow re^{i\delta} \approx \mp\frac{qS_{0+}}{QE_{0+}} \Longrightarrow \frac{qS_{0+}}{QE_{0+}} \approx -\frac{R'^{t}_{LT} \mp iR^{n}_{LT}}{R'^{\ell}_{TT}} \tag{39}$$

provides the ratio of scalar and transverse multipoles as a complex number that is relevant to tests of chiral perturbation theory. The same result should be obtained from both parallel and antiparallel kinematics if the truncation is valid. If this option is activated, the response functions functions are projected to parallel and/or antiparallel kinematics using either the Legendre or the multipole fit and S_{0+}/E_0 is estimated according to Eq. (39). Error propagation is performed using the covariance matrix. Multipole fits using pseudodata based upon realistic models should be used to evaluate the accuracy of this truncation for specified kinematics before accepting the results fit to actual experimental data.

3.7.3. Estimators for S_{0+}/M_{1+} and S_{1+}/M_{1+}

In the immediate vicinity of m_Δ it may be sufficient to approximate

$$W \approx m_\Delta \Longrightarrow re^{i\delta} \approx -\frac{q(S_{0+} \pm 4S_{1+} \pm S_{1-})}{QM_{1+}} \tag{40}$$

Then by comparing parallel and antiparallel kinematics, we can isolate

$$\frac{qS_{0+}}{QM_{1+}} \approx \left(\frac{R'^{t}_{LT} + iR^{n}_{LT}}{2R'^{\ell}_{TT}}\right)_{x=-1} - \left(\frac{R'^{t}_{LT} - iR^{n}_{LT}}{2R'^{\ell}_{TT}}\right)_{x=+1} \tag{41a}$$

$$\frac{q(4S_{1+} + S_{1-})}{QM_{1+}} \approx -\left(\frac{R'^{t}_{LT} + iR^{n}_{LT}}{2R'^{\ell}_{TT}}\right)_{x=-1} - \left(\frac{R'^{t}_{LT} - iR^{n}_{LT}}{2R'^{\ell}_{TT}}\right)_{x=+1} \tag{41b}$$

using polarization measurements. If this option is activated, these ratios are evaluated using response functions functions projected to parallel and/or antiparallel kinematics. Error propagation is performed using the covariance matrix. Multipole fits using pseudodata based upon realistic models should be used to evaluate the accuracy of this truncation for specified kinematics before accepting the results fit to actual experimental data. Unfortunately, it appears that this method is not sufficiently accurate for $p(\vec{e}, e'\vec{p})\pi^0$ for $Q^2 \sim 1$ (GeV$/c)^2$. Nor is S_{1-} negligible. When possible, direct multipole fits to angular distributions are preferred. Nevertheless, the option for this type of analysis remains available.

3.7.4. Target polarization in parallel kinematics

The transformations

$$R^{n}_{LT} \longrightarrow -R^{n}_{LT} \tag{42a}$$

$$R'^{t}_{LT} \longrightarrow \pm R'^{t}_{LT} \tag{42b}$$

$$R'^{\ell}_{TT} \longrightarrow \pm R'^{\ell}_{TT} \tag{42c}$$

allow the formulas in this section to be applied for target polarization observables when the nucleon emerges parallel or antiparallel to $\vec{q}$.

4. AMPLITUDES

The reaction amplitudes for any $A(e, e'N)B$ process where A has spin-$\frac{1}{2}$ and B spin-0 that is governed by the one-photon exchange mechanism can be expressed in terms of *helicity amplitudes* of the form

$$\mathcal{H}_{\lambda_f \lambda_i \lambda_\gamma}(W, Q^2, \theta, \phi) = \langle \lambda_f | \mathcal{F}_\mu \varepsilon^\mu | \lambda_i, \lambda_\gamma \rangle \tag{43}$$

where λ_i and λ_f are the initial and final helicities of the nucleon, λ_γ is the helicity of the virtual photon, $\mathcal{F}^\mu$ is an appropriately normalized transition current operator, and ε^μ is the virtual-photon polarization vector. Since parity conservation [18] requires $|\mathcal{H}_{-\lambda_f -\lambda_i -\lambda_\gamma}| = |\mathcal{H}_{\lambda_f \lambda_i \lambda_\gamma}|$, it is sufficient to consider six independent amplitudes $\mathcal{H}_i$ for $(\lambda_f, \lambda_i, \lambda_\gamma)$ chosen as $(-\frac{1}{2}, -\frac{1}{2}, 1)$, $(-\frac{1}{2}, \frac{1}{2}, 1)$, $(\frac{1}{2}, -\frac{1}{2}, 1)$, $(\frac{1}{2}, \frac{1}{2}, 1)$, $(\frac{1}{2}, \frac{1}{2}, 0)$, and $(\frac{1}{2}, -\frac{1}{2}, 0)$ and numbered sequentially [19, 20]. The most general current operator for pseudoscalar meson production consistent with parity conservation and other symmetries can be represented in term of CGLN amplitudes [21, 22] as

$$i\mathcal{F}^0 = \frac{q}{\omega}\left(\mathcal{F}_5'\vec{\sigma}\cdot\hat{q} + \mathcal{F}_6'\vec{\sigma}\cdot\hat{p}\right) \tag{44a}$$

$$i\vec{\mathcal{F}} = \mathcal{F}_1\vec{\sigma} - i\mathcal{F}_2\vec{\sigma}\cdot\hat{p}\vec{\sigma}\times\hat{q} + \mathcal{F}_3\hat{p}\vec{\sigma}\cdot\hat{q} + \mathcal{F}_4\hat{p}\vec{\sigma}\cdot\hat{p} + \mathcal{F}_5\hat{q}\vec{\sigma}\cdot\hat{q} + \mathcal{F}_6\hat{q}\vec{\sigma}\cdot\hat{p} \tag{44b}$$

where

$$\mathcal{F}_5' = \mathcal{F}_5 + \mathcal{F}_3\hat{p}\cdot\hat{q} + \mathcal{F}_1 \tag{45a}$$

$$\mathcal{F}_6' = \mathcal{F}_6 + \mathcal{F}_4\hat{p}\cdot\hat{q} \tag{45b}$$

are combinations which simplify the multipole analysis. Using phases for helicity states following the conventions of Jacob and Wick [18], the helicity amplitudes are related to CGLN coefficients by

$$\mathcal{H}_1 = -e^{i\phi}\sqrt{2}\sin\theta\cos\left(\frac{\theta}{2}\right)(\mathcal{F}_3+\mathcal{F}_4) \tag{46a}$$

$$\mathcal{H}_2 = \sqrt{2}\left(\cos\left(\frac{\theta}{2}\right)(\mathcal{F}_2-\mathcal{F}_1) + \sin\theta\sin\left(\frac{\theta}{2}\right)(\mathcal{F}_3-\mathcal{F}_4)\right) \tag{46b}$$

$$\mathcal{H}_3 = e^{2i\phi}\frac{1}{\sqrt{2}}\sin\theta\sin\left(\frac{\theta}{2}\right)(\mathcal{F}_3-\mathcal{F}_4) \tag{46c}$$

$$\mathcal{H}_4 = \sqrt{2}\left(\sin\left(\frac{\theta}{2}\right)(\mathcal{F}_1+\mathcal{F}_2) + \sin\theta\cos\left(\frac{\theta}{2}\right)(\mathcal{F}_3+\mathcal{F}_4)\right) \tag{46d}$$

$$\mathcal{H}_5 = \frac{Q}{\omega}\cos\left(\frac{\theta}{2}\right)(\mathcal{F}_5'+\mathcal{F}_6') \tag{46e}$$

$$\mathcal{H}_6 = e^{i\phi}\frac{Q}{\omega}\sin\left(\frac{\theta}{2}\right)(\mathcal{F}_5'-\mathcal{F}_6') \tag{46f}$$

where θ and ϕ refer to the meson.

CGLN amplitudes can be expanded in terms of *multipole amplitudes* as follows [22].

$$\mathcal{F}_1 = \sum_\ell \left(\ell M_{\ell+} + E_{\ell+}\right)P_{\ell+1}'(x) + \left((\ell+1)M_{\ell-} + E_{\ell-}\right)P_{\ell-1}'(x) \tag{47a}$$

$$\mathcal{F}_2 = \sum_\ell \left((\ell+1)M_{\ell+} + \ell M_{\ell-}\right)P_\ell'(x) \tag{47b}$$

$$\mathcal{F}_3 = \sum_\ell \left(E_{\ell+} - M_{\ell+}\right)P_{\ell+1}''(x) + \left(E_{\ell-} + M_{\ell-}\right)P_{\ell-1}''(x) \tag{47c}$$

$$\mathcal{F}_4 = \sum_\ell \left(M_{\ell+} - E_{\ell+} - M_{\ell-} - E_{\ell-}\right)P_\ell''(x) \tag{47d}$$

$$\mathcal{F}_5' = \sum_\ell (\ell+1)L_{\ell+}P_{\ell+1}'(x) - \ell L_{\ell-}P_{\ell-1}'(x) \tag{47e}$$

$$\mathcal{F}_6' = \sum_\ell \left(\ell L_{\ell-} - (\ell+1)L_{\ell+}\right)P_\ell'(x) \tag{47f}$$

The multipole amplitudes can be projected from CGLN amplitudes using [19]

$$
\begin{aligned}
M_{\ell+} &= \frac{1}{2(\ell+1)}\int_{-1}^{1} dx\ \left[P_\ell\mathcal{F}_1 - P_{\ell+1}\mathcal{F}_2 + \frac{1}{2\ell+1}(P_{\ell+1}-P_{\ell-1})\mathcal{F}_3\right] &\text{(48a)}\\
M_{\ell-} &= \frac{1}{2\ell}\int_{-1}^{1} dx\ \left[-P_\ell\mathcal{F}_1 + P_{\ell-1}\mathcal{F}_2 - \frac{1}{2\ell+1}(P_{\ell+1}-P_{\ell-1})\mathcal{F}_3\right] &\text{(48b)}\\
E_{\ell+} &= \frac{1}{2(\ell+1)}\int_{-1}^{1} dx\ \left[P_\ell\mathcal{F}_1 - P_{\ell+1}\mathcal{F}_2 - \frac{\ell}{2\ell+1}(P_{\ell+1}-P_{\ell-1})\mathcal{F}_3 + \frac{\ell+1}{2\ell+3}(P_\ell - P_{\ell+2})\mathcal{F}_4\right] &\text{(48c)}\\
E_{\ell-} &= \frac{1}{2\ell}\int_{-1}^{1} dx\ \left[P_\ell\mathcal{F}_1 - P_{\ell-1}\mathcal{F}_2 + \frac{\ell+1}{2\ell+1}(P_{\ell+1}-P_{\ell-1})\mathcal{F}_3 + \frac{\ell}{2\ell-1}(P_\ell - P_{\ell-2})\mathcal{F}_4\right] &\text{(48d)}\\
L_{\ell+} &= \frac{1}{2(\ell+1)}\int_{-1}^{1} dx\ \left[P_\ell\mathcal{F}_5' + P_{\ell+1}\mathcal{F}_6'\right] &\text{(48e)}\\
L_{\ell-} &= \frac{1}{2\ell}\int_{-1}^{1} dx\ \left[P_\ell\mathcal{F}_5' + P_{\ell-1}\mathcal{F}_6'\right] &\text{(48f)}
\end{aligned}
$$

where $x = \cos\theta_\pi$. One must distinguish carefully between longitudinal amplitudes, $L_{\ell\pm}$, and scalar amplitudes, $S_{\ell\pm}$, that are related by

$$\omega S_{\ell\pm} = q L_{\ell\pm} \tag{49}$$

where ω and q are in the cm frame.

Often it is useful to express multipole amplitudes in terms of *partial-wave helicity amplitudes* [19] according to

$$
\begin{aligned}
M_{\ell+} &= [2A_{\ell+} - (\ell+2)B_{\ell+}]\,/\,[2(\ell+1)] &\text{(50a)}\\
E_{\ell+} &= [2A_{\ell+} + \ell B_{\ell+}]\,/\,[2(\ell+1)] &\text{(50b)}\\
S_{\ell+} &= C_{\ell+}/(\ell+1) &\text{(50c)}\\
M_{\ell-} &= [2A_{\ell-} + (\ell-1)B_{\ell-}]\,/(2\ell) &\text{(50d)}\\
E_{\ell-} &= [-2A_{\ell-} + (\ell+1)B_{\ell-}]\,/(2\ell) &\text{(50e)}\\
S_{\ell-} &= -C_{\ell-}/\ell &\text{(50f)}
\end{aligned}
$$

where

$$
\begin{aligned}
A_{\ell+} &= \frac{1}{2}\left[\ell M_{\ell+} + (\ell+2)E_{\ell+}\right] &\text{(51a)}\\
B_{\ell+} &= E_{\ell+} - M_{\ell+} &\text{(51b)}\\
C_{\ell+} &= (\ell+1)S_{\ell+} &\text{(51c)}\\
A_{\ell-} &= \frac{1}{2}\left[(\ell+1)M_{\ell-} - (\ell-1)E_{\ell-}\right] &\text{(51d)}\\
B_{\ell-} &= E_{\ell-} + M_{\ell-} &\text{(51e)}\\
C_{\ell+} &= -\ell S_{\ell-} &\text{(51f)}
\end{aligned}
$$

differ from the usual Hebb-Walker convention [20] by using $S_{\ell\pm}$ in place of $L_{\ell\pm}$.

Finally, resonant contributions to partial-wave helicity amplitudes are often represented in the isobar bar model in terms of *electromagnetic helicity amplitudes* $A_{1/2}(Q^2)$, $A_{3/2}(Q^2)$, $S_{1/2}(Q^2)$ and a Breit-Wigner factor $f(W)$ according to

$$
\begin{aligned}
A_{\ell\pm}(W,Q^2) &= \mp C^I_{\pi N} f(W) A_{1/2}(Q^2) &\text{(52a)}\\
B_{\ell\pm}(W,Q^2) &= \pm C^I_{\pi N} f(W) A_{3/2}(Q^2)\left[\frac{16}{(2j-1)(2j+3)}\right]^{1/2} &\text{(52b)}\\
C_{\ell\pm}(W,Q^2) &= \mp C^I_{\pi N} f(W) S_{1/2}(Q^2) &\text{(52c)}
\end{aligned}
$$

where $C^I_{\pi N}$ is a nonstandard isospin recoupling coefficient defined by PDG [23]. Note that our definition of $C_{\ell\pm}$ differs from most in being based upon $S_{1/2}$ instead of $C_{1/2}$. PDG employs a Breit-Wigner factor of the form

$$f(W) = \left[\frac{q_0}{k} \frac{1}{\pi(2j+1)} \frac{m_N}{W_R} \Gamma_{\pi N} \right]^{1/2} \frac{W_R}{W_R^2 - W^2 - iW_R\Gamma} \tag{53}$$

where $\Gamma = \Gamma(W)$ is an energy-dependent width. However, because one many finds many parametrizations of the width and of electromagnetic phase-space factors in the literature, we employ this parametrization only to relate electromagnetic and partial-wave helicity amplitudes at $(W \to W_R, Q^2 \to 0)$ for input purposes and use a more flexible parametrization, described in Sec. 5.1.2 for other kinematical conditions.

The response functions can be expressed most simply in terms of helicity amplitudes $H_i(W,Q^2,\theta) = \mathcal{H}_i(W,Q^2,\theta,0)$ for $\phi = 0$. Results for recoil polarization are given in Eq. (54) while those for target polarization are given in Eq. (55). These responses are expressed in the *internal* convention employed by `EPIPROD` and were derived independently, but similar formulas can be found in [11]. Although there is considerable redundancy between the sets of response functions for recoil or target polarization, neither set is sufficient by itself to determine the set of helicity amplitudes completely.

The internal response functions for recoil polarization, using the cm reaction basis, are expressed in terms helicity amplitudes as follows.

$$\begin{aligned}
\mathcal{W}_L &= |H_5|^2 + |H_6|^2 && \text{(54a)}\\
\mathcal{W}_L^{n,0} &= -2\mathrm{Im} H_5 H_6^* && \text{(54b)}\\
\mathcal{W}_T &= \left(|H_1|^2 + |H_2|^2 + |H_3|^2 + |H_4|^2\right)/2 && \text{(54c)}\\
\mathcal{W}_T^{n,0} &= \mathrm{Im}\left(H_1 H_3^* + H_2 H_4^*\right) && \text{(54d)}\\
\mathcal{W}_{LT} &= \mathrm{Re}\left((H_1 - H_4)H_5^* - (H_2 + H_3)H_6^*\right) && \text{(54e)}\\
\mathcal{W}_{LT}^{n,0} &= \mathrm{Im}\left((H_4 - H_1)H_6^* - (H_2 + H_3)H_5^*\right) && \text{(54f)}\\
\mathcal{W}_{LT}^{\ell,0} &= \mathrm{Im}\left((H_1 + H_4)H_5^* - (H_2 - H_3)H_6^*\right) && \text{(54g)}\\
\mathcal{W}_{LT}^{t,0} &= \mathrm{Im}\left((H_2 - H_3)H_5^* + (H_1 + H_4)H_6^*\right) && \text{(54h)}\\
\mathcal{W}_{LT}' &= \mathrm{Im}\left((H_4 - H_1)H_5^* + (H_2 + H_3)H_6^*\right) && \text{(54i)}\\
\mathcal{W}_{LT}'^{n,0} &= \mathrm{Re}\left((H_4 - H_1)H_6^* - (H_2 + H_3)H_5^*\right) && \text{(54j)}\\
\mathcal{W}_{LT}'^{\ell,0} &= \mathrm{Re}\left((H_2 - H_3)H_6^* - (H_1 + H_4)H_5^*\right) && \text{(54k)}\\
\mathcal{W}_{LT}'^{t,0} &= \mathrm{Re}\left((H_3 - H_2)H_5^* - (H_1 + H_4)H_6^*\right) && \text{(54l)}\\
\mathcal{W}_{TT} &= \mathrm{Re}\left(H_2 H_3^* - H_1 H_4^*\right) && \text{(54m)}\\
\mathcal{W}_{TT}^{n,0} &= \mathrm{Im}\left(H_1 H_2^* + H_3 H_4^*\right) && \text{(54n)}\\
\mathcal{W}_{TT}^{\ell,0} &= \mathrm{Im}\left(H_2 H_3^* - H_1 H_4^*\right) && \text{(54o)}\\
\mathcal{W}_{TT}^{t} &= \mathrm{Im}\left(H_3 H_4^* - H_1 H_2^*\right) && \text{(54p)}\\
\mathcal{W}_{TT}'^{\ell,0} &= \left(|H_3|^2 + |H_4|^2 - |H_1|^2 - |H_2|^2\right)/2 && \text{(54q)}\\
\mathcal{W}_{TT}'^{t,0} &= \mathrm{Re}\left(H_1 H_3^* + H_2 H_4^*\right) && \text{(54r)}
\end{aligned}$$

Similarly, the internal response functions for target polarization, using the reaction basis, are expressed in terms helicity amplitudes as follows. Note that several differ only in sign from responses for recoil polarization.

$$
\begin{aligned}
\mathcal{W}_{L}^{0,n} &= -\mathcal{W}_{L}^{n,0} && \text{(55a)}\\
\mathcal{W}_{T}^{0,n} &= -\mathcal{W}_{TT}^{n,0} && \text{(55b)}\\
\mathcal{W}_{LT}^{0,n} &= -\mathcal{W}_{LT}^{n,0} && \text{(55c)}\\
\mathcal{W}_{LT}^{0,z} &= \mathrm{Im}\left((H_3 - H_2)H_6^* - (H_1 + H_4)H_5^*\right) && \text{(55d)}\\
\mathcal{W}_{LT}^{0,m} &= \mathrm{Im}\left((H_2 - H_3)H_5^* - (H_1 + H_4)H_6^*\right) && \text{(55e)}\\
\mathcal{W}_{LT}^{\prime n} &= -\mathcal{W}_{LT}^{\prime n} && \text{(55f)}\\
\mathcal{W}_{LT}^{\prime z} &= \mathrm{Re}\left((H_2 - H_3)H_6^* + (H_1 + H_4)H_5^*\right) && \text{(55g)}\\
\mathcal{W}_{LT}^{\prime m} &= \mathrm{Re}\left((H_3 - H_2)H_5^* + (H_1 + H_4)H_6^*\right) && \text{(55h)}\\
\mathcal{W}_{TT}^{0,n} &= -\mathcal{W}_{T}^{n,0} && \text{(55i)}\\
\mathcal{W}_{TT}^{0,z} &= \mathrm{Im}\left(H_1 H_4^* + H_2 H_3^*\right) && \text{(55j)}\\
\mathcal{W}_{TT}^{0,m} &= \mathrm{Im}\left(H_1 H_3^* - H_2 H_4^*\right) && \text{(55k)}\\
\mathcal{W}_{TT}^{\prime 0,z} &= \left(|H_1|^2 - |H_2|^2 + |H_3|^2 - |H_4|^2\right)/2 && \text{(55l)}\\
\mathcal{W}_{TT}^{\prime 0,m} &= -\mathrm{Re}\left(H_1 H_2^* + H_3 H_4^*\right) && \text{(55m)}
\end{aligned}
$$

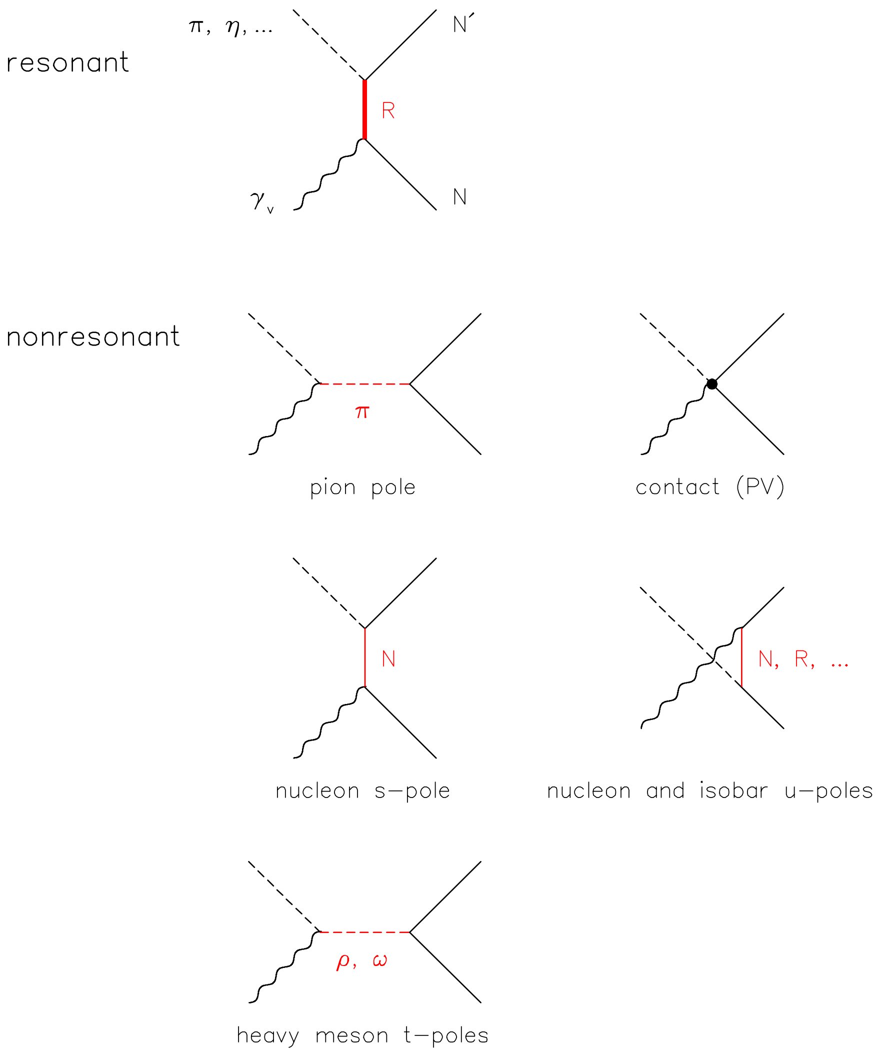

FIG. 2: Resonant and nonresonant diagrams for isobar models.

5. MODELS

5.1. Isobar model

The tree-level diagrams for the isobar model of pion production are shown in Fig. 2. Note that the contact diagram is present only for pion charge exchange with pseudovector coupling and that, at present, we do not include isobar exchange in the u-channel.

5.1.1. Nonresonant diagrams

The electromagnetic vertices are represented by effective lagrangians of the form

$$\mathcal{L}_{\gamma NN} = -e\bar{N}\left[F_1(Q^2)\gamma_\mu\mathcal{A}^\mu + F_2(Q^2)\frac{\sigma_{\mu\nu}}{2m_N}(\partial^\mu\mathcal{A}^\nu)\right]N \tag{56a}$$

$$\mathcal{L}_{\gamma\pi\pi} = e\left[(\partial_\mu\boldsymbol{\pi})^\dagger\times\boldsymbol{\pi}\right]_3\mathcal{A}^\mu F_\pi(Q^2) \tag{56b}$$

where N represents a nucleon field operator, A^μ is the electromagnetic vector potential, and $\boldsymbol{\pi}$ the pion field.

For an isovector meson the meson-pole diagram is represented by an effective lagrangian of the form

$$\mathcal{L}_{\pi NN} = a_{PV}\mathcal{L}^{PV}_{\pi NN} + a_{PS}\mathcal{L}^{PS}_{\pi NN} \tag{57a}$$

$$\mathcal{L}^{PV}_{\pi NN} = -\frac{g^{PV}_{\pi NN}}{2m_N}\bar{N}\gamma_5\gamma_\mu\boldsymbol{\tau}\cdot(\partial^\mu\boldsymbol{\pi})N \tag{57b}$$

$$\mathcal{L}^{PS}_{\pi NN} = ig^{PS}_{\pi NN}\bar{N}\gamma_5\boldsymbol{\tau}\cdot\boldsymbol{\pi}N \tag{57c}$$

where $\mathcal{L}^{PV}_{\pi NN}$ represents pseudovector and $\mathcal{L}^{PS}_{\pi NN}$ pseudoscalar πNN coupling. Following Drechsel *et al.* [24], we provide for mixed PV/PS coupling that interpolates between PV coupling at small p_π and PS coupling at large p_π according to

$$a_{PV} = 1 - a_{PS} = \frac{\Lambda^2_{PV}}{\Lambda^2_{PV} + k^2} \,. \tag{58}$$

This affects only real parts of 0+ and 1− multipoles. For PV coupling we must also include a contact or "seagull" diagram of the form

$$\mathcal{L}_{\gamma\pi NN} = -e\frac{g^{PV}_{\pi NN}}{2m_N}F_A(Q^2)\bar{N}\gamma_5(\boldsymbol{\tau}\otimes\boldsymbol{\pi})_3\,\not{A}N \tag{59}$$

where F_A is the nucleon axial form factor. This diagram only contributes to E_{0+} for the $n\pi^+$ and $p\pi^-$ channels. The coefficient a_{PV} is applied when using mixed coupling.

Similarly, for an isoscalar meson we use

$$\mathcal{L}_{\eta NN} = a_{PV}\mathcal{L}^{PV}_{\eta NN} + a_{PS}\mathcal{L}^{PS}_{\eta NN} \tag{60a}$$

$$\mathcal{L}^{PV}_{\eta NN} = -\frac{g^{PV}_{\eta NN}}{2m_N}\bar{N}\gamma_5\gamma_\mu(\partial^\mu\eta)N \tag{60b}$$

$$\mathcal{L}^{PS}_{\eta NN} = ig^{PS}_{\eta NN}\bar{N}\gamma_5\eta N \tag{60c}$$

where η represents the η-meson field. Although no interpolation between PS and PV has yet been proposed for η production, we provide the same interpolation scheme as for π production; however, we expect that the user will normally choose a nonzero coupling constant for only one of the lagrangians.

Vector-meson diagrams use effective lagrangians of the form

$$\mathcal{L}_{\gamma\pi V} = e\frac{\lambda_V}{m_\pi}\varepsilon_{\mu\nu\alpha\beta}(\partial^\mu A^\nu)\pi_3\partial^\alpha(\delta_{i,3}\omega^\beta + \rho^\beta_i)F_{\gamma\pi V}(Q^2) \tag{61a}$$

$$\mathcal{L}_{\gamma\eta V} = e\frac{\lambda_V}{m_\eta}\varepsilon_{\mu\nu\alpha\beta}(\partial^\mu A^\nu)(\partial^\alpha V^\beta)\eta F_{\gamma\eta V}(Q^2) \tag{61b}$$

$$\mathcal{L}_{VNN} = -\bar{N}\left[\left(g_{V_1}\gamma_\mu + \frac{g_{V_2}}{2m_N}\sigma_{\mu\nu}\partial^\mu\right)(\omega^\nu + \boldsymbol{\tau}\cdot\boldsymbol{\rho}^\nu)\right]NF_{VNN}(t) \tag{61c}$$

where ω^ν and $\boldsymbol{\rho}^\nu$ represent ω and ρ fields, λ_V is an electromagnetic coupling determined by the $V \to \pi\gamma$ radiative decay, and

$$F_{\gamma\pi V}(Q^2) = \left(1 + \frac{Q^2}{\Lambda^2_{\gamma\pi V}}\right)^{-1} \tag{62}$$

is a monopole electromagnetic form factor. Normally one takes $\Lambda_{\gamma\pi V} \to m_V$. A strong form factor,

$$F_{VNN}(t) = \frac{\Lambda^2_{VNN} - m^2_V}{\Lambda^2_{VNN} - t} \tag{63}$$

is applied to the VNN vertex according to the prescription of Brown *et al.* [25].

TABLE II: Generalized Walker parametrizations

Reference	resonance	amplitudes	a_λ	b_λ	c_λ	d	X_π	X_γ
Walker [20]	P_{33}		2	1	0	0	0.16	0.16
	P_{11}		2	1	0	0	0.35	0.35
	D_{13}		2	1	0	0	0.35	0.35
	S_{11}		2	1	0	0	0.35	0.35
	F_{15}		4	2	0	0	0.35	0.35
	D_{15}		4	2	0	0	0.35	0.35
MAID [24]	P_{33}	M_{1+}	4	2	2	-1	0.5	0.5
		E_{1+}, S_{1+}	2	2	2	-1	0.5	0.5
	P_{11}	M_{1-}	2	2	2	-1	0.5	0.5
	D_{13}	M_{2-}	8	2		-1	0.5	0.5
		E_{2-}	4	2		-1	0.5	0.5
	$S_{11}(1535)$	E_{0+}	6	2		-1	0.5	0.5
	$S_{11}(1650)$	E_{0+}	8	2		-1	0.5	0.5
	F_{15}	M_{3-}	8	2		-1	0.5	0.5
		E_{3-}	6	2		-1	0.5	0.5
	D_{33}	M_{2-}	8	2		-1	0.5	0.5
		E_{2-}	8	2		-1	0.5	0.5

5.1.2. Parametrization of resonances

We employ a relativistic Breit-Wigner parametrization of resonant amplitudes. Let $A_{\lambda\pi}(W,Q^2)$ represent an electroproduction amplitude for the $\gamma_\lambda \to R \to \pi N$ transition and let $\bar{A}_{\lambda\pi} = \mathrm{Im}A_{\lambda\pi}(W_R,0)$ represent the imaginary part of the photoproduction amplitude at resonance, $W = W_R$. Here γ_λ refers to a virtual photon either by helicity or partial wave while π represents the meson produced, whether it is a pion or other meson. Thus, we parametrize the resonant amplitude as follows.

$$\frac{A_{\lambda\pi}}{\bar{A}_{\lambda\pi}} = \sqrt{f_\pi}\frac{W_R\Gamma_R e^{i\phi_\lambda}}{W_R^2 - W^2 - i\Gamma W_R}\sqrt{f_\lambda}G_\lambda(Q^2) \tag{64}$$

The factors f_λ and f_π contain phase space and barrier penetrability factors normalized to unity at $(W = W_R, Q^2 = 0)$. The electroexcitation form factor $G_\lambda(Q^2)$ should also be normalized to unity at $Q^2 = 0$. Although many parametrizations appear in the literature, the following generalization of the Walker parametrization [20] of the energy-dependent partial decay width is sufficiently general for most cases.

$$\frac{\Gamma_\pi}{\bar{\Gamma}_\pi} = \frac{k}{k_R}f_\pi = \left(\frac{k}{k_R}\right)^{2\ell_\pi+1}\left(\frac{k_R^2+X_\pi^2}{k^2+X_\pi^2}\right)^{\ell_\pi}\left(\frac{W}{W_R}\right)^d \tag{65}$$

Similarly, the photoexcitation amplitudes are parametrized according to

$$\frac{\Gamma_\lambda}{\bar{\Gamma}_\lambda} = \frac{q_0}{q_{0R}}f_\lambda = \left(\frac{q_0}{q_{0R}}\right)^{a_\lambda}\left(\frac{q_{0R}^2+X_\gamma^2}{q_0^2+X_\gamma^2}\right)^{b_\lambda}\left(\frac{q}{q_R}\right)^{c_\lambda} \tag{66}$$

where the exponents depend upon the particular resonance and may be different for magnetic, electric, and scalar amplitudes.

The total hadronic width usually contains one or more two-body final states with appreciable branching ratios as well as multiparticle final states. At present we employ a relatively simple parametrization based upon Ref. [24]

$$\Gamma = \Gamma_{in} + \sum_{j=1}^{n}\Gamma_j \tag{67}$$

where the resonant widths are

$$\bar{\Gamma}_j = \beta_j\bar{\Gamma} \tag{68a}$$

$$\bar{\Gamma}_{in} = \bar{\Gamma} - \sum_{j=1}^{n}\bar{\Gamma}_j \tag{68b}$$

The energy dependence of partial widths for two-body states is given by Eq. (65) using the meson mass m_j appropriate to channel j, while the energy dependence of the inelastic width is parametrized by

$$\frac{\Gamma_{in}}{\bar{\Gamma}_{in}} = \left(\frac{k_{2\pi}}{\bar{k}_{2\pi}}\right)^{2\ell_\pi+4} \left(\frac{\bar{k}_{2\pi}^2 + X_\pi^2}{k_{2\pi}^2 + X_\pi^2}\right)^{\ell_\pi+2} \tag{69}$$

where $k_{2\pi}$ being the momentum of a composite system with mass $2m_\pi$ and $\bar{k}_{2\pi}$ is evaluated at $W = W_R$.

Several methods are available for parametrizing the resonant amplitudes. If one has a model, such as a quark model, which provides form factors for the electromagnetic helicity amplitudes $A_{1/2}$, $A_{3/2}$, and $S_{1/2}$ it is appropriate to choose `amplitude_type` = `'pwhamps'`. In this case, the phase space factors and form factors will be applied using Eq. (64) interpreting $\{\bar{A}_\lambda, i = 1, 3\}$ as $\{A_{\ell\pm}, B_{\ell\pm}, C_{\ell\pm}\}$. Alternatively, many analyses are performed by applying form factors to multipole amplitudes; hence, if `amplitude_type` = `'mpamps'` then $\{\bar{A}_\lambda, i = 1, 3\}$ are interpreted as $\{M_{\ell\pm}, E_{\ell\pm}, S_{\ell\pm}\}$. In either case, one can choose common or different form factors $G_\lambda(Q^2)$ for each of the three amplitudes. The phase space factors can be chosen individually also.

MAID98 [24] also applies phases $\phi_\lambda(W, Q^2)$ to various multipole amplitudes that are intended to unitarize the resonant contributions. Those phases have been implemented in `epiprod`, primarily for comparisons with MAID98, but are obsolete — later versions of MAID use more sophisticated unitarization procedures and multipole amplitudes for the MAID2003 and DMT [5, 26] models can be read from external files provided by Tiator. Furthermore, we have implemented the somewhat independent unitary isobar model (UIM) described in the next section.

5.2. Unitary isobar model

We use a unitarization prescription suggested by Olssen [27] in which the Born amplitudes are interpreted as contributions to the K-matrix while isobar contributions are unitarized separately using an empirical phase. This procedure is applied to the multipole amplitudes for isospin states. Thus, each multipole amplitude is expressed in the form

$$A = (1 + it)B + Re^{i\psi} \tag{70}$$

where B is the Born contribution described in Sec. 5.1.1, t is the πN partial-wave amplitude, R is a Breit-Wigner resonance parametrized according to Sec. 5.1.2, and ψ is an energy-dependent phase. Angular momentum and isospin labels have been suppressed for brevity.

In our implementation, we evaluate Born amplitudes for both neutral and charged pion production first and then form the combinations needed to obtain isospin amplitudes. The Born multipole amplitudes are determined by numerical integration over the angular distribution of CGLN amplitudes. After recombination with the πN partial-wave amplitudes, we find the following unitarized Born multipoles for each charge state.

$$B_{p\pi^0} \longrightarrow B_{p\pi^0}[1 + \frac{i}{3}(t_{1/2} + 2t_{3/2})] + B_{n\pi^+}[i\frac{\sqrt{2}}{3}(t_{1/2} - t_{3/2})] \tag{71a}$$

$$B_{n\pi^+} \longrightarrow B_{p\pi^0}[i\frac{\sqrt{2}}{3}(t_{1/2} - t_{3/2})] + B_{n\pi^+}[1 + \frac{i}{3}(2t_{1/2} + t_{3/2})] \tag{71b}$$

$$B_{n\pi^0} \longrightarrow B_{n\pi^0}[1 + \frac{i}{3}(t_{1/2} + 2t_{3/2})] + B_{p\pi^-}[-i\frac{\sqrt{2}}{3}(t_{1/2} - t_{3/2})] \tag{71c}$$

$$B_{p\pi^-} \longrightarrow B_{n\pi^0}[-i\frac{\sqrt{2}}{3}(t_{1/2} - t_{3/2})] + B_{p\pi^-}[1 + \frac{i}{3}(2t_{1/2} + t_{3/2})] \tag{71d}$$

$$\tag{71e}$$

The unitarity phase for isobar contributions is adjusted according to the Fermi-Watson theorem [28], which requires

$$Re^{i\psi} = \pm|R|e^{i\delta} \tag{72}$$

where δ is the πN elastic phase shift for the appropriate partial wave. At present we assume that δ is real and have not provided for inelasticity effects above the 2π threshold. The unitarity phases differ for each multipole and are dependent upon the background parametrization. If MAID98 phases are included in the resonance parametrizations, as described in Sec. 5.1.2, they are superceded by the phase used here whenever the `UIM` model is employed. If several resonances are present in a particular partial wave, the unitarization is applied to the net multipole amplitude summed over resonances.

We are presently using the SAID FA02 solutions for πN partial-wave amplitudes [29] for the purposes of unitarization. Special care is needed for the P_{11} partial wave because at low energies it exhibits an extra loop in the Argand diagram. Therefore, the sign ambiguity in Eq. (72) is resolved for $1-$ multipoles by adding π to δ for the P_{11} partial wave at low energies.

6. PROGRAM

6.1. Organization

The program is written in Fortran and has been tested on several Unix systems, including DEC-Alpha, Linux, SunOS, and HP. VMS is no longer supported.

The program consists of:

`epiprod.f`
: The main program is short, simply reading the basic mode of operation and calling the appropriate subprogram. This file and the associated makefile should be in the top source directory for the program.

include files
: Several files contained in the `INCLUDE` subdirectory contain parameter and variable specifications and common blocks. The dimensions of most arrays are based upon parameters rather than explicit values. The user can then modify these parameters and all related dimensions should be adjusted automatically.

`epiprod_lib`
: The bulk of the code is contained in the subdirectory `LIB`. Most source files contain several closely related subprograms. These sources are compiled and linked into an object library as directed by the makefile in this subdirectory. Other programs, such as Monte Carlo simulations, can access `epiprod` routines by linking with this library. There is little danger that common blocks will conflict with other codes, but it may be necessary to rename some of the subprograms.

`JJKLIB`
: `EPIPROD` also uses an external library, named `jjklib.a`, containing a large collection of numerical and service routines that are also employed by several of my other programs.

6.2. Files

Most of the basic I/O files are identified by environment variables in the shell script that initiates the program. A typical script is reproduced below. Not all environment variables are active for all modes. In this particular script, `DATA` defines the location of data files and is used within input files for fitting routines. Similarly, `epidir` is environment variable that points to the `EPIPROD` top directory; normally it would be defined by your login script.

```
#!/bin/csh

setenv input_file       $1.inp
setenv output_file      $1.out
setenv plot_file        $1.plt
setenv DATA             $epidir/SAMPLES

setenv data_plt         "$1_data.plt"
setenv obs_plt          "$1_obs.plt"
setenv rsfns_plt        "$1_rsfns.plt"
setenv rsfns_fit        "$1_rsfns.fit"
setenv legendre_coeffs  "$1_legendre_coeffs.plt"
setenv mpamps_plt       "$1_mpamps.plt"
setenv mpamps_base      "$1_mpamps.base"
setenv para_plt         "$1_para.plt"

$epidir/epiprod.exe
```

These variables are described below.

TABLE III: Columns in plot files.

file							
data_plot	W	Q^2	ϵ	$x_{\rm cm}$ or θ_N or θ_π	ϕ_N or ϕ_π	value	uncertainty
obs_plot	W	Q^2	ϵ	$x_{\rm cm}$ or θ_N or θ_π	ϕ_N or ϕ_π	value	uncertainty
rsfns_plot	W	Q^2	ϵ	$x_{\rm cm}$ or θ_N or θ_π	value	uncertainty	
legendre_coeffs	W	Q^2	coefficient	uncertainty			
mpamps_plt	W	Q^2	amplitude	uncertainty			
mpamps_base	W	Q^2	amplitude				
para_plot	W	Q^2	ϵ	$x_{\rm cm}$	value	uncertainty	

`input_file` The basic input file for specifying the mode of operation, options, kinematics, and model parameters.

`output_file` Detailed output is written to this file with formatting intended for ease of reading. Sections with column formatted could be extracted as input to plotting software, but several additional output files containing subsets of the output are provided in a more directly plottable form.

`plot_file` Contains response functions, observables, azimuthal asymmetries, helicity amplitudes and other quantities evaluated on a simple one dimensional grid.

`data_plot` This reports the data used for fitting. The data output is not necessarily identical to the data input. For example, if one fits Legendre coefficients, the output reports nominal (grid) values for $x_{\rm cm}$ while the output for multipole fits reports acceptance-averaged $\langle x_{\rm cm} \rangle$.

`obs_plot` Calculated or fitted distributions of cross sections and polarization observables on a $(W, Q^2, x_{\rm cm}, \phi)$ grid. The output grid may be finer than the data grid.

`rsfns_plot` Calculated or fitted distributions of response functions on a $(W, Q^2, x_{\rm cm}, \phi)$ grid. The output grid may be finer than the data grid.

`rsfns_fit` Used by `fitmode = 'rsfns'` to report response functions fitted to ϕ and ϵ dependence of cross section and polarization data.

`legendre_coeffs` Tables of fitted Legendre coefficients.

`mpamps_plt` Tables of fitted multipole amplitudes.

`mpamps_base` Tables of baseline multipole amplitudes used to initialize multipole amplitudes and constrain higher partial waves.

`para_plot` The quantities described in Sec. 3.7 pertaining to R_L/R_T for parallel kinematics.

The plot files typically contain many blocks of output where each block begins with a label identifying the tabulated quantity. The next line specifies the number of lines in the table and the number of columns (if greater than 2). A simple one-dimensional grid will then have two columns of x, y where x is the independent kinematical quantity and y is the corresponding observable, response function, amplitude, or other quantity. The next block follows immediately thereafter with its label. The plotting software needs to scan the file for the appropriate label and retrieve the desired tables. Some plot files contain blocks with more than two columns; their column order is listed in Table III.

6.3. Input conventions

Most of the input uses free format, indicated by the `(*)` format specifier. It is not necessary to count columns and the variables read by an input list can be spaced for visual clarity and can be spread over several lines, if desired. Most options are read as character variables within single quotes and are case sensitive. A free-format input list is terminated by a slash (`/`) with subsequent unread variables unchanged. Therefore, options are initialized with default values and are not changed unless valid input is supplied. Invalid input will usually produce a warning message. The calculation will sometimes proceed with default options.

File names are read either on a single line in `(A)` format or in free `(*)` format, as indicated below. Free format is used when it is desired to associate additional variables, such as quantity name or input option, with the data to obtained from that file. The file name is then enclosed by single quotes and read in `(*)` format together with its associated options in a single input list. Alternatively, we sometimes read the file name on a single line without using quotes; note that blank lines or extraneous space is not permitted under those circumstances. File names beginning with `$` are identified as environment variables and are interpreted using `getenv`.

6.4. Standard variables

Energies are in GeV, momenta in GeV/c, masses in GeV/c^2, and angles in degrees. The units for cross sections and response functions can be either microbarn or fm.

Many of the options and variables are common to several modes of operation. Here we provide definitions for common variables.

6.4.1. Options for observables and response functions

The conventions used for observables and response functions, such as polarization basis and kinematical factors, are read in a single input list of character variables that must be terminated by a slash (`/`). The ordering of these options is arbitrary and omitted options remain at default settings. Avoid entering more than one selection for each option – if several are entered, the last will be used. Not all options are relevant for all modes. Inclusion of irrelevant but valid options has no adverse effect, but unrecognized options will generate warning messages. The input is case sensitive. The available options are listed in Table IV with default settings and the recognized choices.

Calculations of observables are normally performed using the internal conventions for response functions, but an option for using the external response functions is provided for testing purposes. This option is selected by including `'use external'` in the options list, but is only active in the `'exclusive'` mode.

Finally, if the list of options includes `'quad'` and the mode is `project_mpamps` or `project_leg`, quadrupole ratios will be evaluated for $N \to \Delta$ excitation. Specifically, Eq. (20) is evaluated for `project_mpamps` or Eq. (21) for `project_leg`. Be aware, however, that these formulas are only relevant for $W \approx m_\Delta$.

6.4.2. Print and plot options

Some types of output to the main output file or to files intended for use by plotting programs can be enabled or disabled using character variables that are interpreted as toggle switches. For example, if we read a print option of the form `'print stuff'` the desired stuff will be printed if it is one of the choices listed in Table V. Similarly, a plot option of the form `'plot stuff'` produces output in a form suitable for plotting programs. Unrecognized stuff has no effect and omitted stuff reverts to default choices. Output can be suppressed for observables or response functions, whose defaults are to both print and plot, using options similar to `'no print rsfns'`.

All print options are read from an input list terminated by a slash. The plot options are read from the next input list, also slash-terminated. Not all items are relevant for all modes of operation. The ordering within each list is irrelevant but the input is case sensitive.

6.4.3. Kinematical variables

Direct calculations are often made on a uniform grid for one of the hadronic variables with the other three held fixed. The independent variable is selected by `hvar` from the choices listed in Table VI. The grid is then specified by `v1min, v1max, v1inc` where `v1min` is the minimum and `v1max` the maximum value of that variable; note that `v1max` is required to be greater than or equal to `v1min`. The spacing is determined

TABLE IV: Options for observables and response functions.

option	default	choices	description
opt_pol	'recoil'	'recoil'	recoil polarization
		'target'	target polarization
pol_basis	'cm reaction'		basis for recoil polarization
		'cm reaction'	(t, n, ℓ) basis, Eq. (7)
		'photon'	(x, y, z) basis, Eq. (8)
		'lab reaction'	(S, N, L) basis, Eq. (9)
		'polarimeter'	(d, e, f), Eq. (10)
		'lab'	(a, b, c), Eq. (11)
		'reaction'	(m, n, z) basis, Eq. (12)
pol_basis	'reaction'		basis for target polarization
		'reaction'	(m, n, z) basis, Eq. (12)
		'photon'	(x, y, z) basis, Eq. (8)
		'lab'	(a, b, c), Eq. (11)
pol_ldir	'pol l=pnuc'	'pol l=pnuc'	$\hat{\ell} = \hat{p}_N$ for recoil polarization
		'pol l=ppi'	$\hat{\ell} = \hat{p}_\pi$
rsfns_ldir	'rsfns l=pnuc'	'rsfns l=pnuc'	$\hat{\ell} = \hat{p}_N$ for response functions
		'rsfns l=ppi'	$\hat{\ell} = \hat{p}_\pi$
		'rsfns l=qvec'	$\hat{\ell} = \hat{q}$
rsfns_type	'standard'	See Table I	conventions for response functions
opt_R	'not reduced'	'not reduced'	response functions according to Eq. (13)
		'reduced'	response functions according to Eq. (14)
opt_theta	'xcm'	'xcm'	$x_{\rm cm}$ used in grids and output for fits
		'theta_pi'	θ_π used in grids and output for fits
		'theta_p'	θ_N used in grids and output for fits
opt_phi	'phi_pi'	'phi_pi'	ϕ_π used in grids and output for fits
		'phi_p'	ϕ_N used in grids and output for fits
rsfns_units	'ub'	'ub'	response functions in microbarns/sr
		'fm'	response functions in fm^2/sr
mpamps_units	'sqrt(ub)'	'sqrt(ub)'	multipole amplitudes printed in $(\mu b)^{1/2}$
		'10^-3/mpi+'	multipole amplitudes printed in $10^{-3}/m_{\pi+}$

TABLE V: Print and plot options. Options of the form 'print stuff' or 'plot stuff' produce output for quantities labeled 'stuff' if that is a valid choice from this table.

stuff	defaults	description
obs	print, plot	observables like cross section and polarization
rsfns	print, plot	response functions
hamps	no output	helicity amplitudes
asymm	no output	azimuthal asymmetries for selected quantities
lcoeff	no output	Legendre coefficients
xcoeff	no output	coeffcients of x^n
mpamps	no output	multipole amplitudes

by `v1inc`, where a positive value specifies an increment while the absolute value of a negative input specifies the number of points.

The next line gives fixed values for the remaining hadronic variables from the ordered list $\{W, Q^2, \theta, \phi\}$. For example, if θ varies on a grid, the constant kinematics are read in the order $\{W, Q^2, \phi\}$. If `hvar` is a nucleon angle, θ_N or ϕ_N, the next line provides the other member of this pair; similarly, if `hvar` is a meson angle, the next line also provides the other meson angle. For this purpose `xcm` is considered a meson angle. If `hvar` is either `'W'` or `'Q2'`, the angles `theta` and `phi` are interpreted according to the `opt_theta` and `opt_phi`, respectively. Thus, `theta` specifies θ_N, θ_π, or x_{cm} when `opt_theta` is `theta_p`, `theta_pi`, or `xcm`. Similarly, `phi` specifies ϕ_N or ϕ_π when `opt_phi` is `phi_p` or `phi_pi`.

If the polar angle is negative, the azimuthal angle is increased by 180°. This permits one to evaluate

TABLE VI: Options for kinematical variables.

variable	choices	description
`hvar`		independent hadronic variable for 1d grid
	`'thcm'`	nucleon polar angle in cm frame
	`'xcm'`	$x_{\rm cm} = \cos\theta_\pi$
	`'thpi'`	pion polar angle in cm frame
	`'phi'`	azimuthal angle in cm frame
	`'W'`	invariant mass
	`'Q2'`	photon virtuality
`evar`		electron kinematical variable
	`'E0'`	beam energy
	`'eps'`	tranverse polarization of virtual photon
	`'theta'`	θ_e

left-right asymmetries within the reaction plane.

The next line specifies the electron scattering kinematics. A quantity specified by `evar`, from the list in Table VI, is held fixed to the value `ekinval` while the remaining dependent variables are computed without further input.

Alternatively, the `grid` mode and the fitting routines use produce output for a four-dimensional grid of (W, Q^2, θ, ϕ) where the intepretation of the θ and ϕ variables is governed by `opt_theta` and `opt_phi`. Thus, the grid for polar angle can be x, θ_N, or θ_π while the azimuthal grid can be ϕ_N or ϕ_π depending upon the options chosen. The grid for each variable is specified in the form

`ny,dy,y0` $\Longrightarrow y_i = y_0 + (i-1) * dy, \qquad i = 1, ny$

Thus, there must be one or more input lines of the form

$$n_W, dW, W_0,\ n_{Q^2}, dQ^2, Q_0^2,\ n_\theta, d\theta, \theta_0,\ n_\phi, d\phi, \phi_0$$

The `'grid'` mode needs one such line, but fitting routines require two: the first line applies to the fitting parameters and the second to the output. All variables must be present even if some are irrelevant.

6.5. Indices and labels

Sets of related quantities, such as response functions, are often collected in arrays where each quantity is identified by an index parameter rather than an explicit value. These indices are assigned by `PARAMETER` statements in the include files. We strongly recommend that if the user modifies the code, the index should be used by name rather than by value. For example, the $R_{LT}'^{n}$ response function is identified by the label `RLThn` and carries the index `iLThn`, where `h` refers to helicity dependence and `n` identifies the polarization component. Note that the indices for polarization components are selected cyclically from (t, n, ℓ) independent of the options chosen for bases. The component labels for print or plot output are replaced by the appropriate letters from Sections 3.2 or 3.3, such as (m, n, z) for the reaction basis. The same label is used in output files and for reading data.

Indices and labels for the quantities recognized by fitting routines are listed in Table VII. Similar indices and labels exist for azimuthal asymmetries and other quantities, but are not tabulated here because they are not available for input or fitting.

TABLE VII: Indices and labels for observables and response functions that are recognized by fitting routines. The output labels are given for the (t, n, l) basis; the component labels are replaced by the appropriate letters for other bases, such as (m, n, z) for the reaction basis.

quantity	index	label
σ_0	`isig0`	`sigma`
A	`iA`	`anal`
P_t	`iPt`	`Pt`
P_n	`iPn`	`Pn`
P_ℓ	`iPl`	`Pl`
P'_t	`iPht`	`Pht`
P'_n	`iPhn`	`Phn`
P'_ℓ	`iPhl`	`Phl`
R_L	`iL`	`RL`
R_T	`iT`	`RT`
R_{LT}	`iLT`	`RLT`
R_{TT}	`iTT`	`RTT`
R'_{LT}	`iLTh`	`RLTh`
R^n_L	`iLn`	`RLn`
R^n_T	`iTn`	`RTn`
R^n_{LT}	`iLTn`	`RLTn`
R^n_{TT}	`iTTn`	`RTTn`
R'^n_{LT}	`iLThn`	`RLThn`
R^ℓ_{LT}	`iLTl`	`RLTl`
R^ℓ_{TT}	`iTTl`	`RTTl`
R'^ℓ_{LT}	`iLThl`	`RLThl`
R'^ℓ_{TT}	`iTThl`	`RTThl`
R^t_{LT}	`iLTt`	`RLTt`
R^t_{TT}	`iTTt`	`RTTt`
R'^t_{LT}	`iLTht`	`RLTht`
R'^t_{TT}	`iTTht`	`RTTht`
R_{L+T}	`iL_T`	`RL+T`
R^n_{L+T}	`iL_Tn`	`RL+Tn`

7. INPUT FOR DIRECT CALCULATIONS

7.1. Initial input

The main input file is used to specify the mode of operation, kinematic variables, and types of output desired. The initial input is common to all modes of operation. The remainder of the input depends upon the selected mode of operation and is described in subsequent sections. In this and related descriptions, lines of input are separated by ruled lines.

`mode`

Valid modes of operation include:

`'exclusive'` evaluates exclusive electroproduction reactions

`'inclusive'` integrates electroproduction cross section over angles, producing total cross sections as functions of either Q^2 or W

`'grid'` evaluates exclusive electroproduction reactions on a kinematic grid for hadronic variables with up to 4 dimensions

`'project_mpamps'` calculates angular distributions for CGLN coefficients and projects multipole amplitudes using angular integration

`'project_leg'` calculates response functions and projects Legendre coefficients using angular integration

`'mpamps'` tabulates multipole amplitudes for charge states or for various isospin representations `'fit'` several types of fits to data, selected by `fitmode` with the choices:

- `'mpamps'` fits multipole amplitudes
- `'legendre'` fits Legendre expansion coefficients
- `'rsfns'` fits response functions to ϕ and ϵ dependencies of cross section and polarization data

`rsfns_to_obs` evaluates observables from response functions to check internal consistency of a data set

`check_pol` checks consistency of polarization data

`'mceep'` used when `EPIPROD` is called from within `MCEEP`

`reaction`

The valid reactions are listed below with their labels, `reaction`, and an internal index, `irea`.

`irea`	`reaction`	description
1	`'ppi0'`	$\gamma_v + p \to p + \pi^0$
2	`'npi+'`	$\gamma_v + p \to n + \pi^+$
3	`'npi0'`	$\gamma_v + n \to n + \pi^0$
4	`'ppi-'`	$\gamma_v + n \to p + \pi^-$
5	`'peta'`	$\gamma_v + p \to p + \eta$
6	`'neta'`	$\gamma_v + n \to n + \eta$

---

options for polarizations and response functions

See Sec. 6.4.1.

---

print options

See Sec. 6.4.2

---

plot options

See Sec. 6.4.2

7.2. Input for `mode='exclusive'`

In the `'exclusive'` mode distributions are computed on a uniform grid for one of several possible hadronic variables. For any valid choice of independent variable, `hvar`, a uniform grid between minimum and maximum values of that variable is constructed. The next line provides fixed values for the 3 remaining variables needed to completely specify the kinematics of the hadronic side of the reaction. The final line of the kinematics section specifies the fixed value for one of the leptonic variables. Details of this input scheme are described in Sec. 6.4.3.

---

hadronic kinematics

`hvar, v1min, v1max, v1inc`

fixed values for the hadronic variables remaining from $\{W, Q^2, \theta, \phi\}$

See Sec. 6.4.3 for details.

---

electron kinematics

`evar, ekinval`

---

model input

The input describing the model of the reaction now follows, as described in Sec. 9 below.

A simple sample input file is reproduced below. The MAID multipole amplitudes are read from a file and calculations of the angular distribution for recoil polarization in the $p\pi^0$ channel at the Δ resonance are performed using the conventions of Drechsel and Tiator for direct comparison with the output of the MAID webpage [4]. Observables, response functions, and helicity amplitudes are printed on the both main output and the plot file.

```
'exclusive'
'ppi0'
'recoil' 'cm reaction' 'pol l=ppi' 'DT' /
'print obs' 'print rsfns' 'print hamps' 'print asymm' /
'plot obs' 'plot rsfns' 'plot hamps' 'plot asymm' /
'thpi' 0. 180. 10.
1.232 1.0 0.
'eps' 0.95
'read mpamps'
$epidir/PION/MAID2003/maid_mpamps.ppi0
-1 /
```

7.3. Input for `mode='inclusive'`

The inclusive mode integrates cross sections over the entire angular distribution as functions of W or Q^2, with other kinematic variables held constant. The user specifies a grid of W, ω, or Q^2 for the inclusive cross sections and for each set of kinematics the program performs calculations at the angles needed for 20 point Gauss-Legendre integration. Expansions in x^n and/or $P_n(x)$, where $x = \cos\theta_\pi$, are then evaluated according to Eq. (15). The following input controls the generation of angular coefficients.

---

expansion limits: n_T, n_{LT}, n_{TT}

If any of the print or plot options for Legendre or power series expansions are chosen true, we read the polynomial order for R_T, R_{LT}, and R_{TT} where $n_L = n_T$. This line is omitted if all print and plot options are false.

---

hadronic kinematics

`hvar, v1min, v1max, v1inc`

fixed value for the remaining hadronic variable, either W or Q^2

---

electron kinematics

`evar, ekinval`

---

model input

The input describing the model of the reaction now follows, as described in Sec. 9 below.

A sample input file is reproduced below. The MAID multipole amplitudes are read from a file and integrated partial cross sections are evaluated at $Q^2 = 1.0$ (GeV/c)^2 for a range of W. Legendre and power series expansions of the unpolarized response functions are made for $n \leq 3$. Rosenbluth combinations are evaluated for the specified beam energy.

```
'inclusive'
'ppi0'
'standard' /
'print lcoeff' 'print xcoeff' /
'plot lcoeff' 'plot xcoeff' /
 3 3 3
'W' 1.1 1.6 0.02
1.0
'E0' 4.53
'read mpamps'
$epidir/PION/MAID2003/maid_mpamps.ppi0
-1 /
```

7.4. Input for `mode='project_mpamps'`

This mode is useful for evaluating multipole amplitudes for the isobar model or for internal consistency checks. It is also useful for the SAID model because Arndt's subroutines do not provide the multipole amplitudes directly. First we calculate helicity amplitudes, then we convert helicity amplitudes to CGLN amplitudes, and finally we evaluate multipole amplitudes using the angular integrations in Eq. (46). The user specifies a grid of either W or Q^2 for the multipole amplitudes and for each set of kinematics the program computes helicity amplitudes at the angles needed for 20 point Gauss-Legendre integration. The following input controls the generation of multipole amplitudes.

minimum and maximum ℓ for multipoles

kinematics

A uniform grid of either W or Q^2 is specified by `hvar, hmin, hmax, dh`
The next line gives the fixed value for the other hadronic variable.

model input

The input describing the model of the reaction now follows, as described in Sec. 9 below.

The sample file below reads multipole amplitudes for MAID and then computes multipole amplitudes using the projection formulas, thereby testing the accuracy and internal consistency of the algorithm. This particular case evaluates a range of W for constant $Q^2 = 1.0$ (GeV/c)^2. Default options are indicated by lines containing just a slash. The multipole amplitudes are reported in customary units of $10^{-3}/m_{\pi^+}$. The option `'quad'` activates calculation of R_{EM} and R_{SM}.

```
'project_mpamps'
'ppi0'
'10^-3/mpi+' 'quad' /
/
/
0 5
'W' 1.1 1.6 0.01
1.0
'read mpamps'
$epidir/PION/MAID2003/maid_mpamps.ppi0
-1 /
```

7.5. Input for `mode='mpamps'`

This mode produces tables of multipole amplitudes for the four charge states or for several representations of the three independent isospin amplitudes for pion electroproduction. The calculation always begins with the amplitudes for charge states and then forms four linear combinations depending upon the desired output representation. Recogning that only three of the amplitudes are independent if isospin symmetry is respected by the pion electroproduction model, the redundancy provides a useful consistency check. The following representations are available.

isospin 1/2 and 3/2 for p or n targets

$$
\begin{aligned}
{}_pA^{(1/2)} &= (A^{(p\pi^0)} + \sqrt{2}A^{(n\pi^+)})/3 &\quad (73a)\\
{}_nA^{(1/2)} &= (-A^{(n\pi^0)} + \sqrt{2}A^{(p\pi^-)})/3 &\quad (73b)\\
{}_pA^{(3/2)} &= A^{(p\pi^0)} - A^{(n\pi^+)}/\sqrt{2} &\quad (73c)\\
{}_nA^{(3/2)} &= A^{(n\pi^0)} + A^{(p\pi^-)}/\sqrt{2} &\quad (73d)
\end{aligned}
$$

Note that ${}_pA^{(3/2)}$ and ${}_nA^{(3/2)}$ should be redundant if isospin invariance is valid for the model selected, but both are output as a consistency check.

isospin amplitudes

$$
\begin{aligned}
A^{(1/2)} &= (A^{(p\pi^0)} + A^{(n\pi^0)})/2 + (A^{(n\pi^+)} - A^{(p\pi^-)})/\sqrt{2} && \text{(74a)}\\
A^{(0)} &= (A^{(p\pi^0)} - A^{(n\pi^0)})/6 + (A^{(n\pi^+)} + A^{(p\pi^-)})/\sqrt{18} && \text{(74b)}\\
{}_pA^{(3/2)} &= A^{(p\pi^0)} - A^{(n\pi^+)}/\sqrt{2} && \text{(74c)}\\
{}_nA^{(3/2)} &= A^{(n\pi^0)} + A^{(p\pi^-)}/\sqrt{2} && \text{(74d)}
\end{aligned}
$$

crossing amplitudes

$$
\begin{aligned}
A^{(+)} &= (A^{(p\pi^0)} + A^{(n\pi^0)})/2 && \text{(75a)}\\
A^{(-)} &= (A^{(n\pi^+)} - A^{(p\pi^-)})/\sqrt{8} && \text{(75b)}\\
A^{(0)}_{\pm} &= (A^{(n\pi^+)} + A^{(p\pi^-)})/\sqrt{8} && \text{(75c)}\\
A^{(0)}_{0} &= (A^{(p\pi^0)} - A^{(n\pi^0)})/2 && \text{(75d)}
\end{aligned}
$$

The two versions of $A^{(0)}$ should be equal if isospin symmetry is respected.

After reading `mode`, the next 4 standard input items (reaction, options, print options, plot options) are irrelevant but placeholders are still required. The remaining input is described below.

output representation

The first significant item is `type` and is chosen from:

`'charge'` lists amplitudes for charge states

`'p,n,3/2'` lists amplitudes in ${}_pA^{(1/2)}$, ${}_nA^{(1/2)}$, and $A^{(3/2)}$ format

`'isospin'` lists amplitudes in $A^{(1/2)}$, $A^{(0)}$, and $A^{(3/2)}$ format

`'crossing'` lists crossing amplitudes $A^{(+)}$, $A^{(0)}$, and $A^{(-)}$

angular momentum range

`lmin, lmax`

kinematics

A uniform grid of either W or Q^2 is specified by `hvar, hmin, hmax, dh`
The next line gives the fixed value for the other hadronic variable.

model input

The input describing the model of the reaction now follows, as described in Sec. 9 below.

A sample input file is given below, where the W dependence is scanned for fixed $Q^2 = 1.0$ (GeV/c)^2. Note that 4 sets of input are needed when reading multipole amplitudes from an external file because amplitudes for each charge state are read from separate files. Here we use the same units as the MAID web page [4] so that the results can be compared directly. Both `plt` and `out` files have very similar multicolumn formats, but the `plt` file does not label the columns. Plotting software must be told which columns to select.

```
'mpamps'
'ppi0'
'10^-3/mpi+' /
/
/
'p,n,3/2'
0 5
'W' 1.1 1.6 0.01
1.0
```

```
'read mpamps'
$epidir/PION/MAID2003/maid_mpamps.ppi0
-1 /
$epidir/PION/MAID2003/maid_mpamps.npi0
-1 /
$epidir/PION/MAID2003/maid_mpamps.npi+
-1 /
$epidir/PION/MAID2003/maid_mpamps.ppi-
-1 /
```

7.6. Input for mode='project_leg'

The mode expands response functions in Legendre series with coefficients on a uniform grid of either W or Q^2.

---

maximum ℓ

---

kinematics

- A uniform grid of either W or Q^2 is specified by `hvar, hmin, hmax, dh`
- The next line gives the fixed value for the other hadronic variable, either W or Q^2.
- Finally, the electron kinematics are given by `evar, ekinval`, where `evar` is either `'E0'` or `'eps'` and `ekinval` is either the beam energy (GeV) or ϵ.

---

model input
The input describing the model of the reaction now follows, as described in Sec. 9 below.

A sample input file is reproduced below. The MAID multipole amplitudes are read from a file and response functions are evaluated at $Q^2 = 1.0$ (GeV$/c)^2$ for a range of W. Legendre expansions of recoil-polarization response functions using standard conventions are made for $\ell \leq 6$. Rosenbluth combinations are made for the specified beam energy. The option `'quad'` activates calculation of $\tilde{R}_{EM}$ and $\tilde{R}_{SM}$. We chose not to print tables of coefficients but the output is written to the `plot_file` by default.

```
'project_leg'
'ppi0'
'quad' /
'no print lcoeff' /
/
 6
'W' 1.1 1.6 0.01
1.0
'E0' 4.53
'read mpamps'
$epidir/PION/MAID2003/maid_mpamps.ppi0
-1 /
```

7.7. Input for mode='grid'

This mode performs model calculations on a four-dimensional (W, Q^2, x, ϕ) and is useful for comparison with data or for preparation of tables for event generators that use interpolation. However, because the maximum number of points is presently limited by the parameter `mnpts`, it may be necessary to subdivide the grid and then merge the output files later. The output tables are written to `plot_file`.

TABLE VIII: Default tolerances for assigning data to kinematical bins.

quantity	tolerance	unit
W	0.005	GeV
Q^2	0.01	$(\mathrm{GeV}/c)^2$
ϵ	0.002	
x_{cm}	0.001	
θ_{cm}	0.5	deg
ϕ	0.5	deg

electron kinematics
`evar, ekinval`

---

grid parameters for output
Four-dimensional grid specification according to Sec. 6.4.3

---

model input
The input describing the model of the reaction now follows, as described in Sec. 9 below.

A sample input based upon the SAID model is listed below. This file uses $\phi = 0$, which is suitable for tabulation of response functions.

```
'grid'
'ppi0'
/
/
/
'E0' 4.53
10 0.02 1.17  1 0.2 1.0  20 0.10 -0.95  1 0. 0.
'GWU'
```

8. INPUT FOR FITTING PROCEDURES

8.1. Basic input

Several fitting routines are available for the analysis of data in the form of cross sections, polarizations, or response functions. The parameters are assumed to depend upon a subset of the variables (W, Q^2, x, ϕ) that assume values on a uniform grid. For example, because multipole amplitudes or Legendre coefficients depend upon (W, Q^2), parameters are fit on the two-dimensional grid (W_i, Q_j^2) using data with arbitrary values of (x, ϕ). Similarly, response functions can be extracted on a three-dimensional grid of (W_i, Q_j^2, x_k) using data for arbitrary ϕ. Output for plotting purposes is provided upon a four-dimensional grid that might have finer spacings for the independent variables. The grid for each variable is specified in the form
`ny,dy,y0` $\Longrightarrow y_i = y_0 + (i-1) * dy, \qquad i = 1, ny$
Thus, there must be two input lines of the form

$$n_W, dW, W_0,\ n_{Q^2}, dQ^2, Q_0^2,\ n_x, dx, x_0,\ n_\phi, d\phi, \phi_0$$

where the first line applies to the fitting parameters and the second to the output. All variables must be present even if some are irrelevant.

We also require tolerances on the kinematics in data files in order to assign each datum to the proper bin. Thus, there is a line specifying tolerances for $W, Q2, \epsilon, x_{cm}, \theta_{cm}, \phi$. The default values for these tolerances are listed in Table VIII.

The interpretation of the polar and azimuthal angles used in these four-dimensional grids is governed by the variables `opt_theta` and `opt_phi` read in the initial input section.

`opt_theta` governs the polar angle:

> `'xcm'` grids x
>
> `'theta_p'` grids θ_p in cm frame
>
> `'theta_pi'` grids θ_π in cm frame

`ppt_phi` governs the azimuthal angle:

> `'phi_p'` grids ϕ_p
>
> `'phi_pi'` grids ϕ_π

The fitting procedures are based upon the Levenberg-Marquardt algorithm. The search ends when either a maximum number of iterations is performed or when the change in reduced chisquare becomes sufficiently small. Note that by specifying that the maximum number of iterations is zero, the output for the final fit will be the same as the initial fitting function. This can be useful for procedures, such as `'mpamps'`, that are based upon variations with respect to a baseline model.

Several options are available for fitting procedures. These are read as character variables in a single free format list terminated by a slash. The current options are:

- `'pseudodata'`
  Replace input data with pseudodata based upon a model calculation. This is useful for testing the internal consistency of fitting routines or the sensitivity of proposed data to a model parameter. See Sec. 8.9.
- `'quad'`
  Evaluate SMR and EMR for $N \to \Delta(1232)$ using either the truncated Legendre expansion for `fitmode='legendre'` or fitted multipole amplitudes for `fitmode='mpamps'`.
- `'Rparallel'`
  Evaluate R_L/R_T using polarization response functions for parallel kinematics according to Sec. 3.7.1.
- `'S0parallel'`
  Evaluate S_{0+}/E_{0+} using polarization response functions for parallel kinematics assuming s-wave dominance, as discussed in Sec. 3.7.2.
- `'S1parallel'`
  Evaluate S_{1+}/M_{1+} and S_{0+}/M_{1+} using polarization response functions for parallel kinematics assuming M_{1+} dominance, as discussed in Sec. 3.7.3.
- `'skip first'`
  Omit listing of initial fitting function.
- `'skip last'`
  Omit listing of final fitting function.
- `'read param'`
  Read initial fitting parameters from external file.
- `'write param'`
  Write final fitting parameters to external file.
- `'bin ff'`
  Use a form factor to compensate for difference between acceptance-averaged and nominal Q^2.
- `'bin center'`
  Use a model to compensate for differences between acceptance-averaged and nominal (W, Q^2).

The basic input has the following structure. Several items depend upon `fitmode` and are described more fully in subsequent sections.

`fitmode`

---

convergence criteria

`mnfit` maximum number of iterations
`conv` minimum change in reduced chisquare

---

options for fitting procedures

---

grid parameters for data

---

grid parameters for output

---

binning tolerances

---

input parameter file

A file name is read here in `(A)` format for the `'read param'` option and is omitted otherwise.

---

output parameter file

A file name is read here in `(A)` format for the `'write param'` option and is omitted otherwise. Note that two files are needed if both `'read param'` and `'write param'` are chosen.

---

model input for bin centering

A model is needed for the `'bin center'` option; this section is omitted otherwise. The model input is described in Sec. 9.

---

form factor

A model form factor is needed for the `'bin ff'` option; this section is omitted otherwise. We use a modified dipole parametrization

$$G(Q^2) = \frac{1 + aQ^2}{(1 + \frac{Q^2}{\Lambda^2})^2} e^{-bQ^2} \tag{76}$$

and read Λ^2, a, b. The default values are $0.71, 0, 0$ if this input is slash terminated.

---

data files as described in Sec. 8.2.

---

model input for pseudodata

A model is needed here for the pseudodata option; this section is omitted otherwise. The model input is described in Sec. 9.

---

parameter specification

Depends upon `fitmode`; details to follow.

---

model input

A baseline model is needed for `fit_mpamps`, as described in Sec. 9.

---

parameters for projection of baseline multipoles

If the baseline model for `fit_mpamps` is not obtained by reading a file of multipole amplitudes, the baseline multipoles are projected from CGLN coefficients on a (W, Q^2) grid specified here; this section is omitted otherwise. The input consists of the maximum orbital angular momentum and grids for Q^2 then W.

```
lmax
nq_mp, dq_mp, q0_mp
nW_mp, dW_mp, W0_mp
```

TABLE IX: Options for data input.

option	default	choices	description
input_theta	'xcm'	'xcm' 'theta_p' 'theta_pi'	polar angle
input_phi	'phi_pi'	'phi_pi' 'phi_p'	azimuthal angle
input_Rtype	'standard'	See Table I	conventions for response functions
input_red	'reduced'	'reduced' 'not reduced'	response functions according to Eq. (14) response functions according to Eq. (13)
input_kincor	'no center'	'no center' 'center'	no bin centering apply bin centering corrections
input_ekin	'eps'	'eps' 'E0'	electron kinematics given by ϵ electron kinematics given by E_0

8.2. Data files

Most fitting procedures can read data for several different quantities from separate files. At the appropriate place in the input file, one or more lines containing the character variables

`type, datafile, input_theta, input_phi, input_Rtype, input_R, input_kincor`

is entered in free format. Here `type` is a label identifying the quantity tabulated in `datafile`, `datafile` is a file name, and the remaining variables are options for interpreting angular variables and conventions for response functions. A list of recognized quantities is given in Table VII. The ordering of quantities is irrelevant, but a particular quantity may not appear more than once. The list of data files is terminated by `'end' /`.

The input options may be given in any order and assume the defaults listed in Table IX if omitted. Different options can be specified for each input file. Once a value is supplied for one of these options, it becomes the new default until it is possibly reset by a subsequent choice. Therefore, it is convenient to group data files according to their input options. The program stops if an invalid option is encountered. Remember that slash termination is needed if any options are omitted.

If `type='multi'`, data for several quantities can be read from a single internally labeled file and a common set of options applies to the entire file. It is often convenient to include all of the response functions for an experiment in a single file. The data file then contains one or more repetitions of the following sequence:

```
label
nrow ncol
data set
```

where `label` identifies the quantity, `nrow` is the number of rows (data points) for that quantity, and `ncol` is the number of columns in the data set. The number of columns is included for compatibility with auxiliary plotting programs but is ignored by this program.

Each data set contains a sequence of lines where each line contains the 12 columns listed in Table X. The first 7 columns are mandatory. Acceptance-averaged kinematics can be omitted by terminating a line with a slash (/). If acceptance-averaged kinematics are omitted, they are assumed to be equal to the central values of the bin specified by first 5 columns. The columns for ϕ must be present for response functions even though that angle is irrelevant. Similarly, columns for ϵ must also be supplied even when irrelevant.

The output is governed by the options read in the initial input section. Therefore, input data are converted to output conventions before producing output files for plotting purposes.

8.3. Methods for bin centering

Multipole amplitudes and Legendre coefficients are functions of (W, Q^2), but the acceptance averaged $(\overline{W}, \overline{Q^2})$ generally depend upon x_{cm}. Consequently, amplitudes fitted to angular distributions can be distorted by the x_{cm} variations of $(\overline{W}, \overline{Q^2})$. Irregular variations may artificially enhance higher partial waves.

TABLE X: Structure of data files.

column	quantity	description
1	W	invariant mass in GeV
2	Q^2	photon virtuality in $(\text{GeV}/c)^2$
3	ϵ or E_0	chosen by `input_ekin`
4	x or θ	polar angle in cm
5	ϕ	azimuthal angle in degrees
6	experimental value	
7	uncertainty	
8	$\langle W \rangle$	acceptance-averaged W
9	$\langle Q^2 \rangle$	acceptance-averaged Q^2
10	$\langle \epsilon \rangle$ or $\langle E_0 \rangle$	acceptance-averaged ϵ or E_0
11	$\langle x \rangle$	acceptance-averaged x
12	$\langle \phi_\pi \rangle$	acceptance-averaged ϕ_π

Two methods for compensating for such distortions have been implemented and those methods are compared for JLab experiment e91011 in Ref. [30].

The additive method is based upon the first-order expansion

$$f(W,Q^2,\bar{x},\bar{\epsilon}) = f(\overline{W},\overline{Q^2},\bar{x},\bar{\epsilon}) - \frac{\partial f}{\partial W}(\overline{W}-W) - \frac{\partial f}{\partial Q^2}(\overline{Q^2}-Q^2) \tag{77}$$

where f represents any response function or observable (cross section, beam analyzing power, or polarization) and where overlines indicate acceptance averaging and where the derivatives are evaluated at central kinematics using a suitable model, such as MAID.

Additive kinematical corrections have the advantages that variations of both W and Q^2 can be accommodated and corrections can be made to polarizations, but this procedure has the disadvantage that it relies upon a model and we have no model that provides a uniformly good fit to all of the response functions. While that is not a problem for pseudodata, the use of an inaccurate model to make kinematical corrections to real data could introduce more serious errors than it corrects. Therefore, a second procedure based upon form factors was tested. Assuming that all response functions share a common form factor, and that kinematical corrections are dominated by the x_{cm}-dependence of $\overline{Q^2}$, we postulate

$$R(W,Q^2,\bar{x}) = R(\overline{W},\overline{Q^2},\bar{x})\left(G(Q^2)/G(\overline{Q^2})\right)^2 \tag{78}$$

and approximate $G(Q^2)$ by the usual dipole form factor $G_D(Q^2) = (1+Q^2/\Lambda^2)^{-2}$ where $\Lambda^2 = 0.71$ $(\text{GeV}/c)^2$. The multiplicative correction can also be applied to the differential cross section but does not affect polarization data. This multiplicative procedure does not compensate for variations of $\overline{W}$, but those variations are typically much smaller than those for $\overline{Q^2}$ for common binning choices.

In order to evaluate the sensitivity of the kinematical corrections to the choice of form factor, the multiplicative option `'bin ff'` employs the more general Sato-Lee parametrization [6]

$$G(Q^2) = \frac{1+aQ^2}{(1+\frac{Q^2}{\Lambda^2})^2} e^{-bQ^2} \tag{79}$$

where the default values $(\Lambda^2, a, b) = (0.71, 0, 0)$ correspond to the traditional dipole form factor. We usually find that negligible differences between multipole analyses performed using either $N \to \Delta$ or dipole form factors.

Even if bin centering input is supplied, the bin centering option must be activated for each data set before it is applied; see Sec. 8.2. One can choose to activate this option for some data sets, such as response functions, while not activating it for others, such as cross sections that are already projected to nominal kinematics. Note that if either bin centering option is activated, the data reported in output and plot files are modified.

8.4. Input for `fitmode='mpamps'`

The `fitmode='mpamps'` mode is used to fit multipole amplitudes to angular distribution data for response functions. Angular distributions for several different response functions can be analyzed simultaneously, but we assume that all share common fixed values of W and Q^2. Therefore, grid values are used for W and Q^2 while acceptance-averaged values are used for x and ϕ. The bin centering options `'bin ff'` or `'bin center'` can be used to compensate for differences between acceptance-averaged and nominal (W, Q^2). For Rosenbluth combinations we assume that ϵ is independent of angular variables.

We represent helicity amplitudes in the form

$$h_{ij} = h_{ij}^{(0)} + \sum_{k=1}^{n} c_k h_{ijk}^{(1)} \tag{80}$$

where i is an index for the kinematical condition (angle), $1 \leq j \leq 6$ is the amplitude index, and c_k are variable coefficients. Suppose that one wants to vary a particular multipole amplitude, such as S_{1+}, while all other multipole amplitudes remain fixed by a model. One first computes the helicity amplitudes $h_{ij}^{(0)}$ for the invariant part of the model, then computes the helicity amplitudes $h_{ijk}^{(1)}$ produced by each of the variable multipoles using unit strengths. Note that the real and imaginary contributions are separated, so that the parameters c_k are real. By fitting these parameters to data, we obtain the *change* in each amplitude relative to the baseline model. Often it is convenient to nullify the variable multipoles before evaluating the baseline model so that the fitting parameters represent the strength rather than the change in strength for each fitted multipole. This would be done in the section for model input.

Often the baseline model is obtained by reading multipole amplitudes for a theoretical model from a file. Cubic-spline interpolation is then used to obtain the required values of (W, Q^2). Although there is a provision for extrapolation, extrapolation of splines is notoriously unreliable — it is the user's responsibility to verify that the (W, Q^2) ranges in the multipole file span those in the data files so that interpolation is reliable. Alternatively, the baseline model can be one of the internal models. For example, if the baseline model consists of Born terms the fitted parameters would represent resonances plus perhaps changes in background terms due to final-state interactions. The latter could appear as imaginary contributions to nonresonant multipoles. One could also use Breit-Wigner parametrizations of nondominant resonances in order to include the contributions of their tails to the background below the resonances of interest. Under these conditions, it is necessary to compute the multipole amplitudes for the baseline model by integration over angular distributions for CGLN coeffcients on a (W, Q^2) grid large enough to encompass the experimental kinematics. The baseline multipoles can then be added to the fitted parameters to obtain total multipole amplitudes for plotting purposes. The final input section for `'fitmode=mpamps'` specifies the maximum ℓ_π and the (W, Q^2) grid used for this purpose. It does not have to coincide with the data grid, but it should encompass the data grid and it should be fine enough for accurate interpolation. Interpolation is not needed if the two grids do coincide.

There is also a provision for beginning the fit with relatively little freedom, adjusting the most important variables first, and then allowing additional freedom after the initial fit has converged. By entering a value of 2 for `novcs`, two sets of vary codes are read for each (ℓ, j) in the list of variable multipoles. Normally the second set permits more freedom than the first.

The section that specifies the fitting parameters contains the following input for each variable multipole. The list is terminated by $\ell = -1$. Note that for small ℓ entries must be made for forbidden amplitudes, such as M_{0+}.

`novcs`: number of sets of vary codes

ℓ orbital angular momentum

j twice the total angular momentum

---

initial values for parameters
  ReM, ImM, ReE, ImE, ReS, ImS

---

vary codes for initial fit
6 integers: 0 for fixed, 1 for variable

---

vary codes for final fit if `novcs=2`
6 integers: 0 for fixed, 1 for variable

A sample input file based upon JLab experiment e91011 is reproduced below. Data for the differential cross section, beam analyzing power, and reduced response functions are supplied on a 10×1 grid of (W, Q^2). Although acceptance-averaged values are employed for (x, ϕ), the nominal input grids must still be specified. The next slash indicates that default binning tolerances are used. The data for all response functions are collected in a single file of type `'multi'`. The traditional dipole form factor is used to project data for recoil polarization response functions from acceptance-averaged to nominal Q^2; the data cross section and beam analyzing power have already been projected to central kinematics and do not require bin centering corrections here. This particular experiment contained only one beam energy, so the data file includes the Rosenbluth combinations R_{L+T} and R^n_{L+T} but does not contain separated data for R_L, R_T, R^n_L, or R^n_T.

At each grid point two fitting cycles are employed, each allowing up to 100 iterations to reach convergence at the level of $\delta\chi^2 \leq 0.0001$. The baseline model uses Born terms for pseudovector πNN coupling plus vector-meson diagrams. The first cycle optimizes real and imaginary parts of all multipole amplitudes for $\ell_\pi \leq 1$ except $\mathrm{Im} M_{1-}$. The second cycle releases constraints upon real parts of $2-$ amplitudes and attempts to improve upon the first result. Output will be produced for a 99×12 grid of (x, ϕ) for each fitted (W, Q^2).

The parameters represent changes with respect to the baseline model. The final three lines specified the maximum orbital angular momentum and a (W, Q^2) grid for evaluation of baseline multipole amplitudes. For this case, multipole amplitudes are obtained by integration over the angular distributions of CGLN coefficients for the Born model. The baseline multipoles are added to the fitting parameters to produce total amplitudes suitable for plotting.

```
'fit'
'ppi0'
'reduced' /
/
/

'mpamps'
 100 0.0001
'bin ff' 'quad' 'Rparallel' 'S1parallel' 'write param' /
mpfit.par
 0.71 /

   10 0.02 1.17  1 0.2 1.0  20 0.10 -0.95  12 30. 15.
   10 0.02 1.17  1 0.2 1.0  99 0.02 -0.98  12 30. 15.
/

'sigma' '$sigma' /
'anal'  '$anal'  /
'multi' '$rsfns' 'center' /
'end' /

 2
1 3
 0.0 0.0 0.0 0.0 0.0 0.0
  1   1   1   1   1   1
  1   1   1   1   1   1
0 1
 0.0 0.0 0.0 0.0 0.0 0.0
  0   0   1   0   1   0
  0   0   1   1   1   1
1 1
```

```
 0.0 0.0 0.0 0.0 0.0 0.0
  1   0   0   0   1   0
  1   0   0   0   1   1
2 3
 0.0 0.0 0.0 0.0 0.0 0.0
  0   0   0   0   0   0
  1   0   1   0   1   0
2 5
 0.0 0.0 0.0 0.0 0.0 0.0
  0   0   0   0   0   0
  0   0   0   0   0   0
-1 /

'isobar'

'start-born'
'standard'
'GALSTER'  'DIPOLE'
'DIPOLE'   'DIPOLE'
'none'
'diff'
 0. 13.4 0.45
 2
 1 0.769   2.  13. 0.103  0.769 1.5
 0 0.7826 21. -12. 0.314  0.783 1.2
/

'none'

   5
   1  0.10  1.00
  10  0.02  1.17
```

8.5. Input for `fitmode='legendre'`

A sample input file based upon JLab experiment e91011 is listed below. Data for the differential cross section, beam analyzing power, and reduced response functions for recoil polarization are supplied on a 10×1 grid of $\{W, Q^2\}$. Although acceptance-averaged values are employed for $\{x, \phi\}$, the nominal input grids must still be specified. The data for all response functions are collected in a single file of type `'multi'`. The traditional dipole form factor is used to project data for recoil polarization response functions from acceptance-averaged to nominal Q^2; the data cross section and beam analyzing power have already been projected to central kinematics and do not require bin centering corrections here. This particular experiment contained only one beam energy, so we fit the Rosenbluth combinations R_{L+T} and R^n_{L+T} and do not vary R_L, R_T, R^n_L, or R^n_T separately. A maximum of 100 iterations per grid point are permitted to reach convergence at the level of $\delta\chi^2 \leq 0.0001$. The data files use default input options, omitted by slash termination.

The section specifying input parameters consists of 20 lines containing the maximum degree for the Legendre expansion for each of the response functions listed in Table VII. The input order must match the order in that table. It is convenient to terminate each of these lines with a slash (/) followed by the input label as a mnemonic device. For some response functions the maximum degree depends upon W, being larger in the central region where the precision and angular coverage are best and smaller in the wings of the W acceptance. The first column is the default $n_{\max}$ and successive columns, if present, are values for points on the kinematics grid, with W varying most rapidly. Because the data set is just a one-dimensional grid, $n_{\max}$ for large W can be omitted and then reverts to its default.

```
'fit'
'ppi0'
```

```
'reduced' /
/
/

'legendre'
 100 0.0001
'bin ff' 'quad' 'Rparallel' 'S1parallel' /
 0.71 /

   10 0.02 1.17  1 0.2 1.0  20 0.10 -0.95  12 30. 15.
   10 0.02 1.17  1 0.2 1.0  99 0.02 -0.98  12 30. 15.
/

'sigma' '$sigma' /
'anal'  '$anal'  /
'multi' '$rsfns' 'center' /
'end' /

 0 / RL
 0 / RT
 2 2 2 3 3 3 3 3 / RLT
 1 1 1 2 2 2 2 1 / RTT
 2 2 2 3 3 3 3 3 / RLTh
 0 / RLn
 0 / RTn
 3 / RLTn
 2 / RTTn
 3 / RLThn
 3 / RLTl
 2 2 2 3 3 3 3 3 / RTTl
 3 / RLThl
 4 3 3 4 4 4 4 4 3 3 3 / RTThl
 4 / RLTt
 3 / RTTt
 4 / RLTht
 3 / RTTht
 3 3 3 4 4 4 4 4 / RL+T
 2 2 2 3 3 3 3 3 / RL+Tn
```

8.6. Input for `fitmode='rsfns'`

A sample input file is listed below but sample data are not provided. The azimuthal dependence of data for the differential cross section is used to extract the unpolarized response functions R_{LT}, R_{TT}, and the Rosenbluth combination R_{L+T} on a $5 \times 2 \times 40$ grid of $\{W, Q^2, x\}$. Although acceptance-averaged values are employed for ϕ, the nominal input grid must still be specified. Output will be produced for a 181 values for each fitted $\{W, Q^2, x\}$. A maximum of 100 iterations per grid point are permitted to reach convergence at the level of $\delta\chi^2 \leq 0.001$. The initial fitting function is omitted because the initial parameters are essentially meaningless; the fit converges from practically anywhere when there are a sufficient number of ϕ's because the azimuthal dependencies are so simple.

The section specifying input parameters consists of 20 lines containing a vary code for each of the response functions listed in Table VII, where 1 means fit and 0 means omit. Thus, only three response functions can be extracted using only cross section data for a single beam energy. The input order must match the order in that table. It is convenient to terminate each of these lines with a slash (/) followed by the input label as a mnemonic device.

```
'fit'
```

```
'ppi0'
/
/
/

'rsfns'
 100 0.001
'skip first'/

   5 0.04  1.18  2 0.20 0.9   40 0.05 -0.95   12 30. 15.
 100 0.005 1.1   2 0.20 0.9    0 0.02 -1.0   181  2.  0.
/

'sigma' 'sigma.dat' /
'end' /

 0 / RL
 0 / RT
 1 / RLT
 1 / RTT
 0 / RLTh
 0 / RLn
 0 / RTn
 0 / RLTn
 0 / RTTn
 0 / RLThn
 0 / RLTl
 0 / RTTl
 0 / RLThl
 0 / RTThl
 0 / RLTt
 0 / RTTt
 0 / RLTht
 0 / RTTht
 1 / RL+T
 0 / RL+Tn
```

8.7. Input for mode='rsfns_to_obs'

The mode **'rsfns_to_obs'** can be used to check the internal consistency between response functions and polarization observables extracted from the same data. A sample input file is listed below but sample data files are not provided. Data for response functions are read on a $\{W, Q^2, x\}$ grid and polarization observables are computed as a function of ϕ for each $\{W, Q^2, x\}$ point with sufficient information. In this example separate files read for each response functions. The value of n_x for plot output is ignored. Simple error propagation is performed assuming that uncertainties in the input data are uncorrelated. The input for this mode has the same structure as for fitting routines except that search parameters and model input are omitted.

```
'rsfns_to_obs'
'ppi0'
/
/
/

  5 0.04 1.18  2 0.20 0.9   40 0.05 -0.95  12 30. 15.
  5 0.04 1.18  2 0.20 0.9    0 0.02 -1.0   12 30. 15.
```

```
/

'sigma'  $DATA/sigma.dat' /
'RLTh'  '$DATA/rltp.dat'  /
'RLTl'  '$DATA/RLTl.dat'  /
'RLThl' '$DATA/RLThl.dat' /
'RTThl' '$DATA/RTThl.dat' /
'RTTl'  '$DATA/RTTl.dat'  /
'RL+Tn' '$DATA/RL+Tn.dat' /
'RLTn'  '$DATA/RLTn.dat'  /
'RLThn' '$DATA/RLThn.dat' /
'RTTn'  '$DATA/RTTn.dat'  /
'RLTt'  '$DATA/RLTt.dat'  /
'RLTht' '$DATA/RLTht.dat' /
'RTTht' '$DATA/RTTht.dat' /
'RTTt'  '$DATA/RTTt.dat'  /
'end' /
```

8.8. Input for `mode='check_pol'`

This mode is useful for checking the validity of polarization data. It reads polarization data and computes the magnitude of the helicity-independent polarization vector and of the net polarization for two helicity states. A sample input file is listed below but sample data files are not available. The structure is similar to that for fitting routines except that options for response functions, convergence criteria, and descriptions of parameters are omitted. Six data files are required for polarization components.

```
'check_pol'
'ppi0'
/
/
/

  5 0.04 1.18  2 0.20 0.9   40 0.05 -0.95  12 30. 15.
  5 0.04 1.18  2 0.20 0.9    0 0.02 -1.0   12 30. 15.
/

'Pn'  'Pn.dat'  /
'Pl'  'Pl.dat'  /
'Pt'  'Pt.dat'  /
'Phn' 'Phn.dat' /
'Phl' 'Phl.dat' /
'Pht' 'Pht.dat' /
'end' /
```

8.9. Testing a fit using pseudodata

Pseudodata can be used to test the fitting procedures for multipole or Legendre analysis or to evaluate how well one should be able to determine various parameters given data with specified precision and kinematic coverage. If one includes `'pseudodata'` on the fitting options line, the input data are replaced by calculated values based upon that model with normally-distributed fluctuations based upon the experimental uncertainties. This requires an additional input section following the list of data files that defines the model for pseudodata. The fitting parameters are then initialized normally and the pseudodata are analyzed like real data. Thus, if the fitting model is sufficiently complete, the fit should produce $\chi^2_\nu \approx 1$. The uncertainties in fitted parameters and the nature of the covariance matrix can be informative. This information could help decide which parameters a data set can determine or could reveal whether there are strong correlations that cannot be resolved.

A sample input file is listed below. Here the data are replaced by calculations based upon SAID and multipole amplitudes are fit using MAID2003 as the baseline model. All s and p wave amplitudes and the real parts of $2-$ amplitudes are varied. An advantage of using different models for pseudodata and for baseline amplitudes is that one can judge the adequacy of a particular truncation scheme for analyzing realistic data. Alternatively, one can use the same model for both pseudodata and baseline multipoles to test the internal consistency of the code.

```
'fit'
'ppi0'
/
/
/

'mpamps'
 100 0.0001
'pseudodata' /

   10 0.02 1.17  1 0.2 1.0  20 0.10 -0.95  12 30. 15.
   10 0.02 1.17  1 0.2 1.0  99 0.02 -0.98  12 30. 15.
/

'sigma' '$sigma' /
'anal'  '$anal'  /
'multi' '$rsfns' /
'end' /

'GWU'

 1
1 3
 0.0 0.0 0.0 0.0 0.0 0.0
  1   1   1   1   1   1
0 1
 0.0 0.0 0.0 0.0 0.0 0.0
  0   0   1   1   1   1
1 1
 0.0 0.0 0.0 0.0 0.0 0.0
  1   1   0   0   1   1
2 3
 0.0 0.0 0.0 0.0 0.0 0.0
  1   0   1   0   1   0
-1 /

'read mpamps'
$epidir/PION/MAID2003/maid_mpamps.ppi0
-1 /
```

9. MODEL INPUT

The input for model parameters is read from the file identified by the environment variable `input_file` established by the script that runs the program. The model section begins by reading a character variable `model` describing the type of model desired. There are three choices at present.

9.1. SAID

The SAID model [3, 31] is obtained by selecting `model='GWU'` and requires no further input. The helicity amplitudes are obtained from Fortran routines provided by Arndt and Strakovsky; all subsequent manipulations (response functions, observables, mutipole decomposition, etc.) employ standard `epiprod` subroutines. This option is the simplest choice, but it does not allow one to vary any aspect of the model. We are now using the WI03 version of SAID.

9.2. External multipole amplitudes

An external file containing tables of multipole amplitudes produced using a more sophisticated dynamical model can be read by choosing `model = 'read mpamps'`. The next line in the main input file should then be the name of that file. The required amplitudes will be generated by two-dimensional cubic-spline interpolation with respect to (W, Q^2). The relative importance of various multipoles can be tested using a set of optional scale parameters. After reading the file, one can supply one or more lines of the form

```
l,j2, f_Re_M, f_Im_M, f_Re_E, f_Im_E, f_Re_S, f_Im_S
```

where `l` is the orbital and `j2` is twice the total angular momentum. The 6 scale factors are applied to the real and imaginary parts of magnetic, electric, and scalar amplitudes with self-explanatory names. The list of scale factors is terminated either by end-of-file or by `-1 /`.

The first three lines of the multipole file specify the maximum orbital angular momentum, $\ell_{\max}$, grid parameters n_Q, dQ^2, Q_0^2 specifying $Q_j^2 = Q_0^2 + (j-1) * dQ^2$ for $j = 1, n_Q$, and grid parameters n_W, dW, W_0 specifying $W_i = W_0 + (i-1) * dW$ for $i = 1, n_W$. For each allowed multipole one then reads a block containing Re A followed by a block of Im A where each block is arranged as `((A(i,j), j=1,nq), i=1,nw)`. The amplitudes with increasing $\ell = 0, \ell_{\max}$ are arranged in the order $M_{\ell+}, E_{\ell+}, S_{\ell+}, M_{\ell-}, E_{\ell-}, S_{\ell-}$, omitting amplitudes that do not exist. Thus, the first amplitude is E_{0+} because M_{0+} does not exist. At present we read amplitudes for a specific reaction and do not form linear combinations for isospin representations.

The information needed to produce multipole amplitudes in this format has been provided by L. Tiator for the MAID2000 [24, 32], MAID2003 [26], and DMT [5, 33] models and by T.-S.H. Lee for the SL model [6]. We have verified that `EPIPROD` reproduces the $p\pi^0$ results from the MAID and DMT webpages.

9.3. Isobar model

Alternatively, if `model = 'isobar'` the parametrization described in Sec. 5 will be employed. In this case one first reads a file name for the parametrization of nonresonant amplitudes. The nonresonant amplitudes are omitted if this file name is `'none'` or the necessary input is read directly from the main input file if the file name is given as `'start-born'`. Otherwise, the parameters for nonresonant diagrams are obtained from the specified file according to the format described in Sec. 9.3.1. Next, one reads a file name for the parametrization of resonant amplitudes, which are omitted if that name is `'none'` or read from the main input file if that name is `'start-isobars'`. If the name is `'same'`, isobar input is read from the same file as nonresonant input. This version can use MAID98 phases but does not unitarize background amplitudes.

Finally, `model = 'UIM'` corresponds to the unitary isobar model as described in Sec. 5.2. The input is otherwise similar to the nonunitary isobar model.

9.3.1. Born terms

The following table summarizes the input needed for the standard parametrization of nonresonant diagrams.

Line	variables	default	description
1	`modelb`	`'standard'`	selects model for nonresonant diagrams
2	`etype(0)`	`'GALSTER'`	model for G_{En}
	`mtype(0)`	`'DIPOLE'`	model for G_{Mn}
3	`etype(1)`	`'DIPOLE'`	model for G_{Ep}
	`mtype(1)`	`'DIPOLE'`	model for G_{Mp}
4	`atype`	`'none'`	model for G_A
4.1	Λ_A		for `'monopole'` or `'dipole'`
5	`opt_Fpi`		model for F_π
5.1	Λ_π		for `'monopole'`
6	$g^{PS}_{\pi NN}$		pseudoscalar πNN coupling
	$g^{PV}_{\pi NN}$		pseudovector πNN coupling
	Λ_{PV}	0	parameter for interpolation between PV and PS coupling
7	`NV`		number for vector mesons. Line 8 repeated for each.
8	`IV`		isospin = 0 or 1
	m_V		mass
	g_{V1}		vector coupling constant
	g_{V2}		tensor coupling constant
	λ_V		electromagnetic coupling
	$\Lambda_{\gamma\pi V}$		electromagnetic cut-off
	Λ_{VNN}		strong cut-off
9	`use_s`	`'s'`	`'s'` $\Rightarrow$ include s-pole, omit otherwise
	`use_u`	`'u'`	`'u'` $\Rightarrow$ include u-pole, omit otherwise
	`use_t`	`'t'`	`'t'` $\Rightarrow$ include t-pole, omit otherwise
	`use_seagull`	`'seagull'`	`'seagull'` $\Rightarrow$ include seagull, omit otherwise
	`use_omega`	`'omega'`	`'omega'` $\Rightarrow$ include vector mesons, omit otherwise

More information nucleon form factors and about nonstandard models and options will be furnished later.

9.3.2. Parametrization of resonant amplitudes

The input described in this section is repeated for each resonance until a label `'end'` is encountered. The input consists of four subsections: general properties, parametrization of width, parametrization of electromagnetic amplitudes, and parametrization of unitary phases.

9.3.3. General properties

Line	variables	description
1	`label`	name of resonance
	`lr`	orbital angular momentum
	`tr`	twice isospin
	`jr`	twice total angular momentum
2	`modelr`	model for resonant amplitudes (only 'BW' described)
3	W_R	resonance mass
	Γ_R	total hadronic decay width at resonance

9.3.4. Width

Line	variables	description
1	`modelw`	model for width (only `'Walker'` described)
2	`nbranch`	number of significant two-body channels
3	`channel`	meson produced
	β_i	branching fraction
	X_π	damping parameter for width
	`nW`	exponent d from Eq. (65)

Line 3 is repeated for each two-body channel. The channels are presently limited to `'pi'` or `'eta'`.

9.3.5. Electromagnetic amplitudes

First we read the amplitudes $\bar{A}_\lambda$ for $(W = W_R, Q^2 = 0)$. The input for $\bar{A}_\lambda$ depends upon the choice of `amplitude_type`. Electromagnetic helicity amplitudes are conventionally presented in units of $\text{GeV}^{-1/2}$, but `factor` can be used to multiply the input amplitudes by a conversion factor to these units or to manipulate the relative importance of an isobar for testing purposes. Similarly, multipole amplitudes are normally read in units of $\mu\text{b}^{1/2}$ but these input values can be multiplied by a conversion `factor` also. The input for `'mpamps'` is given for charge states while input for `'emhamps'` is given for isospin states.

Line	variables	description
1	`type`	type of input for amplitudes
2	$\bar{A}_{1/2}$, $\bar{A}_{3/2}$, $\bar{S}_{1/2}$, `factor`	for `'emhamps'`; OR
2	$\bar{M}_{l\pm}$, $\bar{E}_{l\pm}$,$\bar{S}_{l\pm}$, `factor`	for `'mpamps'`

Next we read form factor information. The form factors $G_\lambda(Q^2)$ can be applied either to multipole amplitudes $M_{\ell\pm}$, $E_{\ell\pm}$, $S_{\ell\pm}$ for `amplitude_type = 'mpamps'` or to partial-wave helicity amplitudes $A_{\ell\pm}$, $B_{\ell\pm}$, $C_{\ell\pm}$ or `amplitude_type = 'pwhamps'` where $\lambda = 1, 3$ in either case.

Line	variables	description
1	`amplitude_type`	type of form factor
2	`modelq`	form factor model
	X_γ	damping parameter (GeV)
	$a_\lambda, b_\lambda, c_\lambda$	exponents from Eq. (66)
3		model parameters

Lines 2 and 3 are repeated three times, where the input needed on Line 3 depends upon `modelq`. The simplest choice is to use `dipole0`, corresponding to the standard dipole form factor with $\Lambda^2 = 0.71\ (\text{GeV}/c)^2$. If all three G_λ are identical, one can use `modelq='same'` for $\lambda \geq 2$ and omit model parameters. Other valid choices of form factor include:

`'none'` form factor is set to zero to omit resonance

`'point'` form factor is set to unity

`'dipole'` form factor $(1 + \frac{Q^2}{\Lambda_R^2})^{-2}$ with Λ_R read on next line.

`'NL'` Nozawa-Lee parametrization of $N \to \Delta$ form factor

$$F_{N\Delta}(Q^2) = \frac{a + (1-a)\exp{(-Q^2/b)}}{1 + \frac{Q^2}{\Lambda^2}} \tag{81}$$

with a, b, and Λ read on next line [12, 34, 35].

`'BMZ'` BMZ parametrization of $N \to S_{11}(1535)$ form factors (see [36]).

`'DL'` Devenish-Lyth form factors (see [37–39]).

9.3.6. Unitarity phases

The choice `model='UIM'` selects the unitary isobar model described in Sec. 5.2 and uses built-in SAID partial wave amplitudes. Alternatively two obsolete options remain available, at least temporarily, when using `model='isobar'`.

- `'maid98'`
  If `'maid98'` is selected, the MAID98 parametrization detailed in Ref. [24] is applied without further input. Note, however, the phases are selected based upon the resonance name and that the names recognized by this subroutine are: P33(1232), P11(1440), D13(1520), F15(1680), and D33(1700).

- `'constant'`
  If this option is chosen, three constant phases are read on the next line and applied to the magnetic, electric, and scalar multipole amplitudes in order.

9.3.7. Sample isobar input

Below we provide a sample input for the unitary isobar model based upon a qualitative analysis of the multipole amplitudes fit to recoil polarization response functions for $p\pi^0$ across the $\Delta(1232)$ resonance at $Q^2 = 1.0$ (GeV/c)^2 in Ref. [40]. Only the first P_{33} and P_{11} resonances are included because the data were limited to $W \leq 1.35$ GeV; nevertheless, the input below extrapolates to larger W. We used generic nucleon form factors, dipole and Galster, and used a dipole axial form factor with $m_A = 1.0$ GeV. The `'diff'` prescription for the pion form factor uses $F_\pi = F_{1p} - F_{1n}$. The next line specifies pure pseudovector coupling. The vector meson parameters were taken from MAID98 [24]. Delta and Roper widths at resonance were taken from the recent PDG compilation [41], along with the πN branching ratio of 65% for the Roper. Damping and width parameters were also taken from MAID98, which in turn were based upon the Walker model. The line `'none'` indicates that additional phases were not used; they would be irrelevant anyway because the unitarization procedure decides the energy-dependent phases for each multipole. The electromagnetic structure of the resonances was supplied in the form of multipole amplitudes; note that the data are consistent with $M_{1-} \approx 0$ for the Roper at $Q^2 = 1$. Point form factors were used because we are attempting to estimate resonant contributions for a particular value of Q^2 without assuming that the shape of the form factors is known. For similar reasons, we used $c \to 0$ in Eq. (66) whereas MAID uses $c \to 2$ for $\Delta(1232)$, which results in a W-dependent form factor.

```
'project_mpamps'
'ppi0'
/
/
'plot mpamps' /
0 4
'W' 1.08 1.6 0.01
1.0

'UIM'

'start-born'
'standard'
'GALSTER'  'DIPOLE'
'DIPOLE'   'DIPOLE'
'dipole'
 1.0
```

```
'diff'
 0. 13.4 0.45
 2
 1 0.769   2.  13. 0.103  0.769 1.5
 0 0.7826 21. -12. 0.314  0.783 1.2
/

'start-isobars'
'P33(1232)' 1 3 3
'BW'
 1.232 0.120
'Walker'
 1
'pi' 1.0 0.5 -1
'mpamps'
 1.94 -0.0565 -0.133 1.0
'none'
'mpamps'
'point' 0.5 4 2 0
'point' 0.5 4 2 0
'point' 0.5 4 2 0

'P11(1440)' 1 1 1
'BW'
1.440 0.350
'Walker'
1
'pi'  0.65 0.5 -1
'mpamps'
 0.0 0.0 0.26  1.0
'none'
'mpamps'
'point' 0.5 2 2 0
'point' 0.5 2 2 0
'point' 0.5 2 2 0

'end' /
```

9.4. Legacy models

Several additional models used in the earliest versions of `EPIPROD` remain available but have not been maintained carefully as the code evolved and may not still work. Here we provide brief descriptions of those models but advise caution in their use. If any demand develops we might refurbish one or more of these, but it is more likely that most will be deleted.

`'DLvG'` The resonant amplitudes for pion production are based upon fixed-t dispersion relations developed by Devenish and Lyth [37–39] and the nonresonant amplitudes use the parametrization developed by von Gehlen [42] using pseudoscalar coupling.

`'BL'` The Blomqvist-Laget [43] pion photoproduction model used a nonrelativistic time-ordered decomposition of Feynman diagrams for Born terms, with either pseudoscalar or pseudovector coupling, and a fit to the M_{1+} amplitude for the Δ resonance. The ω exchange diagram is included for neutral pion photoproduction.

`'MW'` The Mehrotra-Wright [44] model is an extension of the BL model to electroproduction. Only pseudovector coupling is considered, but several variations of the M_{1+} fit are available.

'D' The Dressler [45] extension of the BL model is similar to that of MW but uses a different prescription for restoration of gauge invariance.

'BMZ' The model of Benmerrouche, Mukhopadhyay, and Zhang [36] describes η electroproduction using an effective Lagrangian. This model will probably be maintained because it is the only one presently available that is specifically designed for η production. Documentation should be provided also, but I have not actually used this model since writing JLab proposal 96-001 [46].

10. USING EPIPROD AS AN EVENT GENERATOR

EPIPROD can be employed as an event generator within Monte Carlo simulation programs by providing suitable initialization and calling sequences. Interfaces have already been provided for MCEEP [47], gengen [48], and PALM. The subroutines init_mceep_mode, init_gengen_mode, or init_palm_mode are used to initialize the model of the reaction and the parameters used by corresponding program. They also initialize parameters used to convert between the systems of units employed by EPIPROD and the simulation program. It should be relatively simple to adapt these interfaces for use with other Monte Carlo programs provided that there are no conflicts between their common blocks.

The appropriate initialization subroutine must be called before the event generation loop. The model input is read from the file identified by the environment variable input_file and output is written to output_file. It should be easy to modify these names if they conflict with environment variables used by the calling program. The desired reaction is read from input_file and then the model is established according to Sec. 9.

Within the event generator one calls

```
      call epiprod_xsec( react, W_in,Q2_in,theta_in,phi_in,
     .                   epsilon,pol_beam,
     .                   sigma_lab,sigma_cm, anal,
     .                   pol0,polh, rr )
```

where the kinematical variables (W, Q^2, θ, ϕ) are given in the first four arguments, epsilon is the transverse polarization of the virtual photon, and pol_beam is the beam polarization in the range $(-1, 1)$. Note that the internal kinematical variables are obtained from the input variables according to

```
      W      = W_in  * units_W
      Q2     = Q2_in * units_Q2
      thcm_N = (theta_in + offset_theta) * units_theta
      phi_N  = (phi_in   + offset_phi  ) * units_phi
```

where the units and offsets are initialized by the interface subroutine.

The output variables are listed below.

- sigma_lab is the five-fold differential cross section in the laboratory frame
- sigma_cm is the two-fold differential cross section in the cm frame,
- anal is the beam analyzing power,
- pol0 is the helicity-independent polarization vector
- polh is the helicity-dependent polarization vector
- rr is an array of response functions ordered according to the indices defined in Table VII.

The interface subroutine is responsible for conversion of cross sections and response functions to the units required by the simulation program.

APPENDIX A: RELATIVISTIC SPIN ROTATION

It is well-known that the spin direction of a particle is affected by a boost that is not parallel to its momentum, a relativistic effect described as *Wigner rotation* or *Wigner-Thomas precession* [7, 8, 49]. However, because a widely cited "pedagogical paper" [50] provides an incorrect description of this effect that was partly responsible for errors in some earlier versions of this program, we summarize here a derivation of the relativistic spin rotation and provide a detailed description of its implementation for the cm $\rightarrow$ lab transformation of polarization observables.

The intrinsic spin of a massive particle is specified in its rest frame. Suppose that $\vec{\sigma}$ is a unit vector that represents the spin orientation in a rest frame. A spacelike spin four-vector is then formed as $s = (0, \vec{\sigma})$ such that $s_\mu s^\mu = -1$ is invariant. Nevertheless, the orientation of the spin is still represented by the original $\vec{\sigma}$. The relationship between spins in frames differing by a boost that is not parallel to the particle's momentum can be determined by transforming each frame to a rest frame of the particle, using a boost parallel to the momentum in that frame, and comparing the orientations of the two rest frames. These orientations differ because nonparallel boosts do not commute.

Consider two frames, S_1 and S_2, that share a common set of axes

$$\hat{z} = \hat{q},\ \hat{y} \propto \hat{q} \wedge \hat{p},\ \hat{x} = \hat{y} \wedge \hat{z} \tag{A1}$$

and differ by a boost in the $\hat{z}$ direction. It is convenient to express four-vectors in the form (E, p_z, p_x) where the y component is superfluous. Thus, the nucleon four-momentum can be expressed as

$$p_1 = m\gamma_1(1, \beta_1 \cos\theta_1, \beta_1 \sin\theta_1) \tag{A2a}$$
$$p_2 = m\gamma_2(1, \beta_2 \cos\theta_2, \beta_2 \sin\theta_2) \tag{A2b}$$

in S_1 and S_2, respectively. Let

$$B_z(\beta) = \begin{pmatrix} \gamma & -\gamma\beta & 0 \\ -\gamma\beta & \gamma & 0 \\ 0 & 0 & 1 \end{pmatrix} \tag{A3}$$

represent a boost along $\hat{z}$ and let

$$R_y(\theta) = \begin{pmatrix} 1 & 0 & 1 \\ 0 & \cos\theta & \sin\theta \\ 0 & -\sin\theta & \cos\theta \end{pmatrix} \tag{A4}$$

represent a rotation about $\hat{y}$.

If the momentum forms an angle θ_1 with the $\hat{z}$ axis of S_1, the transformation

$$T_1 = R_y(-\theta_1) B_z(\beta_1) R_y(\theta_1) \tag{A5}$$

produces a rest frame labelled R_1. Alternatively, we could first use a boost along the $\hat{z}$ axis to transform S_1 to S_2, in which the momentum $\vec{p}_2$ appears at angle θ_2, and then a boost along $\vec{\beta}_2$ to reach another rest frame labelled R_2. Thus, the transformation

$$T_2 = R_y(-\theta_2) B_z(\beta_2) R_y(\theta_2) B_z(-\beta) \tag{A6}$$

where β is the velocity of S_1 relative to S_2 produces rest frame R_2. These are both rest frames of the same particle, so can differ at most by a rotation about their common $\hat{y}$ axis, such that

$$T_2 = R_y(\chi) T_1 \tag{A7}$$

Thus, the angles between spins in S_1 and S_2 can be obtained from the transformation

$$R_y(\chi) = T_2 T_1^{-1} = R_y(-\theta_2) B_z(\beta_2) R_y(\theta_2) B_z(-\beta) R_y(-\theta_1) B_z(-\beta_1) R_y(\theta_1) \tag{A8}$$

Using that fact that successive rotations about the same axis add, it is easier to evaluate

$$R_y(-\Omega) = B_z(\beta_2) R_y(\theta_2) B_z(-\beta) R_y(-\theta_1) B_z(-\beta_1) \tag{A9}$$

where the negative sign for Ω will be convenient for the cm $\to$ lab transformation and where $\Omega = \theta_1 - \theta_2 - \chi$. Direct multiplication and simplification reveals that $T_2 T_1^{-1}$ is indeed a pure rotation and that

$$\tan\theta_2 = \frac{\beta_1 \sin\theta_1}{\gamma(\beta + \beta_1 \cos\theta_1)} \tag{A10}$$

$$\tan\Omega = \frac{\beta \sin\theta_1}{\gamma_1(\beta_1 + \beta \cos\theta_1)} \tag{A11}$$

$$\chi = \theta_1 - \theta_2 - \Omega \tag{A12}$$

These results are quite general and apply to any spin or to any pair of reference frames, although the most common applications are probably to the lab $\leftrightarrow$ cm transformations for spin one-half. Also note that β may be positive or negative.

Suppose that S_1 is the cm frame while S_2 is the lab frame reached by a boost with $\beta > 0$. The momentum appears to rotate forward, such that $\theta_2 < \theta_1$. The spin also appears to rotate forward but by a smaller angle, such that

$$0 \le \Omega \le \theta_1 - \theta_2 \Longrightarrow \chi \ge 0 \tag{A13}$$

In fact, in the nonrelativistic limit

$$\gamma \to 1 \Longrightarrow \chi \to 0 \tag{A14}$$

one finds that the spin rotation angle vanishes. (Note that this result depends upon β being small and applies even if β_1 is not small.) Thus, χ represents the relativistic spin rotation arising from noncommutation of noncolinear boosts. For pion electroproduction with modest q, one typically finds that χ reaches a maximum value of a few degrees at a cm angle $\theta_1 \sim 90^\circ$.

One must take care to distinguish between polarizations expressed with respect to a fixed basis, usually with $\hat{z} = \hat{q}$, and polarizations expressed with respect to a helicity basis

$$\hat{\ell} = \hat{p},\ \hat{n} \propto \hat{q} \wedge \hat{p},\ \hat{t} = \hat{n} \wedge \hat{\ell} \tag{A15}$$

that is tied to the nucleon momentum. Polarization components within the reaction plane are mixed according to

$$P_z^{(2)} = P_z^{(1)} \cos\chi + P_x^{(1)} \sin\chi \tag{A16a}$$

$$P_x^{(2)} = -P_z^{(1)} \sin\chi + P_x^{(1)} \cos\chi \tag{A16b}$$

in the z-basis or

$$P_\ell^{(2)} = P_\ell^{(1)} \cos\Omega - P_t^{(1)} \sin\Omega \tag{A17a}$$

$$P_t^{(2)} = P_\ell^{(1)} \sin\Omega + P_t^{(1)} \cos\Omega \tag{A17b}$$

in helicity bases. Naturally, the same mixing applies to the corresponding response functions. The mixing of helicity components can be quite large even if χ is small simply because the lab angle θ_2 is often much smaller than the cm angle θ_1.

Equation (26) of Ref. [50] should be equivalent to our Eq. (A17), but Dmitrašinović interchanges Ω and χ and obtains small mixing in the helicity basis. The subsequent discussion makes it clear that this is a conceptual mistake, not just a typographical error — he repeatedly claims, erroneously, that in the cm $\leftrightarrow$ lab transformation the rotation of polarization lags behind the rotation of momentum by a small amount ω that is equivalent to χ (even though the formula is more complicated). The sign of the mixing is also incorrect. These errors have since been acknowledged in an erratum [51].

APPENDIX B: POLARIZATION BASES

The calculation of recoil polarization starts with the cm reaction basis labeled $(\hat{t}, \hat{n}, \hat{\ell})$ and uses internal response functions in the same basis. The polarization can then be transformed to the desired output basis

TABLE XI: Transformations between internal responses and output polarizations. NA indicates that a basis is not appropriate or not available for target polarization. The final column lists the coordinate inversions for the option `'pol=lppi'`.

`pol_basis`	T_1 for recoil	T_1 for target	`'pol l=ppi'`
`'cm reaction'`	1	NA	$R_z(\pi)R_y(\pi)$
`'photon'`	$R_z(-\phi_N)R_y(-\theta_{Ncm})$	$R_z(-\phi_N)$	
`'lab reaction'`	$R_y(-\Omega)$	NA	
`'polarimeter'`	$R_z(-\psi)R_y(-\Omega)$	NA	
`'lab'`	$R_y(\theta_q)R_z(-\phi_N)R_y(-\theta_{Nlab}-\Omega)$	$R_y(\theta_q)R_z(-\phi_N)$	
`'reaction'`	$R_y(-\theta_{Ncm})$	1	$R_x(\pi)R_y(\pi)$

TABLE XII: Transformations between external and internal responses.

`rsfns_basis`	T_2
`'l=qvec'`	$R_y(-\theta_{Ncm})$
`'l=ppi'`	$R_z(\pi)R_y(\pi)$

using a matrix T_1; this transformation includes a Wigner rotation if the polarization basis is defined in the lab frame. It is also useful to construct transformation matrices T_2 that relate external response functions to internal response functions; the external response functions may rotate the $\hat{\ell}$ in the $\hat{q}$ direction or be based upon $\hat{p}_\pi$ instead of $\hat{p}_N$. Thus, we use T_1T_2 to obtain output polarizations from external response functions. These transformations are expressed in terms of rotation matrices

$$R_x(\theta) = \begin{pmatrix} 1 & 0 & 0 \\ 0 & \cos\theta & \sin\theta \\ 0 & -\sin\theta & \cos\theta \end{pmatrix} \qquad R_y(\theta) = \begin{pmatrix} \cos\theta & 0 & -\sin\theta \\ 0 & 1 & 0 \\ \sin\theta & 0 & \cos\theta \end{pmatrix} \qquad R_z(\theta) = \begin{pmatrix} \cos\theta & \sin\theta & 0 \\ -\sin\theta & \cos\theta & 0 \\ 0 & 0 & 1 \end{pmatrix} \tag{B1}$$

where for the polarimeter basis we require the projected angle

$$\tan\psi = \tan\phi_N \cos\theta_{Nlab} \tag{B2}$$

The transformation matrices are given in Tables XI and XII.

Similarly, for target polarization the internal response functions are evaluated in the basis labeled $(\hat{m}, \hat{n}, \hat{z})$ and defined by Eq. (12). Transformations to the target bases available for output are also given in Table XI.

[1] R. W. Lourie, Nucl. Phys. **A509**, 653 (1990).
[2] R. W. Lourie, Zeit. Phys. **C 50**, 345 (1991).
[3] R. A. Arndt, W. J. Briscoe, R. L. Workman, and I. I. Strakovsky, `gwdac.phys.gwu.edu`.
[4] D. Drechsel, O. Hanstein, S. S. Kamalov, L. Tiator, and S. N. Yang, `www.kph.uni-mainz.de/MAID`.
[5] D. Drechsel, O. Hanstein, S. S. Kamalov, L. Tiator, and S. N. Yang, `www.kph.uni-mainz.de/maid/dmt`.
[6] T. Sato and T.-S. H. Lee, Phys. Rev. **C 63**, 055201 (2001).
[7] D. R. Giebink, Phys. Rev. **C 32**, 502 (1985).
[8] E. P. Wigner, Rev. Mod. Phys. **29**, 255 (1957).
[9] W. Albrecht *et al.*, Nucl. Phys. **B27**, 615 (1971).
[10] K. Joo *et al.*, Phys. Rev. Lett. **88**, 122001 (2002).
[11] D. Drechsel and L. Tiator, J. Phys. G **18**, 449 (1992).
[12] S. Nozawa, B. Blankleider, and T. S. H. Lee, Nucl. Phys. **A513**, 543 (1990).
[13] C. Mertz *et al.*, Phys. Rev. Lett. **86**, 2963 (2001).
[14] N. F. Sparveris *et al.*, Phys. Rev. **C 67**, 058201 (2003).
[15] J. J. Kelly, Phys. Rev. **C 60**, 054611 (1999).
[16] H. Schmieden and L. Tiator, Eur. Phys. J. **A8**, 15 (2000).
[17] T. Pospischil *et al.*, Phys. Rev. Lett. **86**, 2959 (2001).

[18] M. Jacob and G. C. Wick, Ann. Phys. (N.Y.) **7**, 404 (1959).
[19] H. F. Jones, Il Nuovo Cimento **40A**, 1018 (1965).
[20] R. L. Walker, Phys. Rev. **182**, 1729 (1969).
[21] G. F. Chew, M. L. Goldberger, F. E. Low, and Y. Nambu, Phys. Rev. **106**, 1345 (1957).
[22] P. Dennery, Phys. Rev. **124**, 2000 (1961).
[23] Particle Data Group, Rev. Mod. Phys. **48, II**, S1 (1976).
[24] D. Drechsel, O. Hanstein, S. S. Kamalov, and L. Tiator, Nucl. Phys. **A645**, 145 (1999).
[25] G. E. Brown, M. Rho, and W. Weise, Nucl. Phys. **A454**, 669 (1986).
[26] D. Drechsel, O. Hanstein, S. S. Kamalov, L. Tiator, and S. N. Yang, www.kph.uni-mainz.de/maid/maid2003.
[27] M. G. Olssen, Nucl. Phys. **78**, 55 (1974).
[28] K. M. Watson, Phys. Rev. **95**, 228 (1954).
[29] R. A. Arndt, I. I. Strkovsky, and R. L. Workman, Phys. Rev. **C 66**, 055213 (2002).
[30] J. J. Kelly, www.physics.umd.edu/enp/jjkelly/e91011/Reports/Analysis/mpamps.ps.gz (unpublished).
[31] R. Arndt, W. Briscoe, I. Strakovsky, and R. Workman, arXiv:nucl-th/0301068 (unpublished).
[32] D. Drechsel, O. Hanstein, S. S. Kamalov, L. Tiator, and S. N. Yang, www.kph.uni-mainz.de/maid/maid2000.
[33] S. S. Kamalov, S. N. Yang, D. Drechsel, O. Hanstein, and L. Tiator, Phys. Rev. **C 64**, 032201(R) (2001).
[34] S. Nozawa, B. Blankleider, and T. S. H. Lee, Nucl. Phys. **A513**, 459 (1990).
[35] S. Nozawa, B. Blankleider, and T. S. H. Lee, Nucl. Phys. **A513**, 511 (1990).
[36] M. Benmerrouche, N. C. Mukhopadhyay, and J. F. Zhang, Phys. Rev. **D 51**, 3237 (1995).
[37] R. C. E. Devenish and D. H. Lyth, Nucl. Phys. **B43**, 228 (1972).
[38] R. C. E. Devenish and D. H. Lyth, Phys. Rev. **D 5**, 47 (1972).
[39] R. C. E. Devenish, D. H. Lyth, and W. A. Rankin, Nucl. Phys. **B59**, 237 (1973).
[40] J. J. Kelly *et al.*, to be submitted to PRC (unpublished).
[41] S. Eidelmann *et al.* (Particle Data Group), Phys. Lett. **B 592**, 1 (2004).
[42] G. von Gehlen, Nucl. Phys. **B9**, 17 (1969).
[43] I. Blomqvist and J. M. Laget, Nucl. Phys. **A280**, 405 (1977).
[44] S. Mehrotra and L. E. Wright, Nucl. Phys. **A362**, 461 (1981).
[45] E. T. Dressler, Can. J. Phys. **66**, 279 (1988).
[46] J. J. Kelly *et al.*, Recoil Polarization in η Electroproduction, TJNAF Proposal 96-001, 1996.
[47] P. E. Ulmer, www.physics.odu.edu/~ulmer/mceep/mceep.html.
[48] J. J. Kelly, www.physics.umd.edu/enp/e93038/gengen.htm (unpublished).
[49] H. P. Stapp, Phys. Rev. **103**, 425 (1956).
[50] V. Dmitrašinović, Phys. Rev. **C 47**, 2195 (1993).
[51] V. Dmitrašinović, Phys. Rev. **C 71**, 059901(E) (2005).